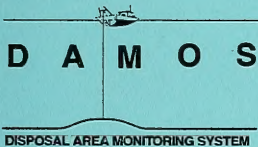
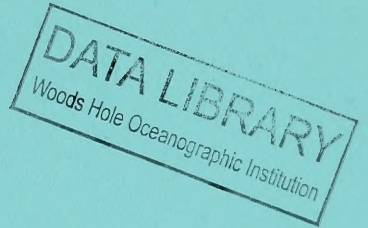

Oceanographic Measurements
at the Portland
Disposal Site
During Spring of 1996

Disposal Area Monitoring System DAMOS



Contribution 121
May 1998



**US Army Corps
of Engineers®**

New England District

TC
187
057
171

REPORT DOCUMENTATION PAGE

form approved
OMB No. 0704-0188

Public reporting concern for the collection of information is estimated to average 1 hour per response including the time for reviewing instructions, searching existing data sources, gathering and measuring the data needed and correcting and reviewing the collection of information. Send comments regarding this burden estimate or any other aspect of this collection of information including suggestions for reducing this burden to Washington Headquarters Services, Directorate for Information Operations and Reports, 1215 Jefferson Davis Highway, Suite 1204, Arlington VA 22202-4302 and to the Office of Management and Support, Paperwork Reduction Project (0704-0188), Washington, D.C. 20503.

1. AGENCY USE ONLY (LEAVE BLANK)		2. REPORT DATE May 1998	3. REPORT TYPE AND DATES COVERED FINAL REPORT	
4. TITLE AND SUBTITLE OCEANOGRAPHIC MEASUREMENTS AT THE PORTLAND DISPOSAL SITE DURING SPRING OF 1996			5. FUNDING NUMBERS	
6. AUTHOR(S) Scott E. McDowell and Stephen D. Pace				
7. PERFORMING ORGANIZATION NAME(S) AND ADDRESS(ES) Science Applications International Corporation 221 Third Street Newport, RI 02840			8. PERFORMING ORGANIZATION REPORT NUMBER SAIC No. 388	
9. SPONSORING/MONITORING AGENCY NAME(S) AND ADDRESS(ES) US Army Corps of Engineers-New England District 696 Virginia Rd Concord, MA 01742-2751			10. SPONSORING/MONITORING AGENCY REPORT NUMBER DAMOS Contribution #121	
11. SUPPLEMENTARY NOTES Available from DAMOS Program Manager, Regulatory District USACE-NAE, 696 Virginia Rd, Concord MA 01742-2751				
12a. DISTRIBUTION/AVAILABILITY STATEMENT Approved for public release; distribution unlimited			12b. DISTRIBUTION CODE	
13. ABSTRACT <p>Under the Disposal Area Monitoring System (DAMOS) Program for the U.S. Army Corps of Engineers, New England District, Science Applications International Corporation (SAIC) conducted an Oceanographic Measurement Program at the Portland Disposal Site (PDS). A single instrumented tripod was deployed from February 27 to May 14, 1996, in order to acquire site-specific data on tides and near-bottom currents, water temperature, and turbidity. The tripod was deployed in the southwest corner of the PDS, in a region of relatively rough topography having a water depth of approximately 60 m. Overall, the 78-day measurement program provided excellent data from which to characterize near-bottom currents and turbidity, and evaluate the physical processes governing bottom sediment resuspension within the PDS.</p> <p>Vertical profiles of temperature, salinity, and density were acquired at a single location in the PDS during February, April, and May 1996, respectively. The February profile revealed a water column that was very weakly stratified, as is typical for the coastal Gulf of Maine in winter. Water property characteristics during late April and mid-May illustrated that relatively fresh and warm water had been introduced to the surface layer, presumably as a result of river discharge. Beneath a moderate thermocline and pycnocline, water properties were nearly constant throughout the lower half of the water column during late spring. With regard to the vertical density stratification, it is apparent that the entire water column to a depth of 60 m is very weakly stratified throughout winter and early spring, whereas the introduction of relatively fresh/warm waters at the surface during mid-spring causes considerable stratification that may tend to decouple horizontal currents and other transport processes within a two-layer water column.</p> <p>Time series observations of winds, waves, atmospheric pressure, and surface water temperatures were acquired from NOAA buoy 44007, located 6 km southwest of the PDS, to assess the seasonal and inter-annual variability in meteorological conditions from 1993 through 1995, as well as meteorological conditions during the 1996 measurement program. Analysis of the annual wave statistics revealed that wave characteristics were very similar for the 3.4 years of wave records. Significant wave heights less than 2 m occurred from 90 to 95% of the time during each year. The maximum significant wave height observed in each of the four measurement years ranged from 5.6 to 7.3 m. Overall, wave characteristics during the first half of 1996 were typical of other recent years at this location.</p> <p>Quantitative analysis of storm waves revealed 72 events during the 3.4-year analysis period that had significant wave heights between 3 and 4 m; average durations for these wave events were only 6 to 8 hrs. Wave heights in the range of 5 to 6 m were observed only 22 times with average durations of less than 3 hrs.</p> <p>The wave records from March through May 1996 exhibited nine storm events attaining significant wave heights greater than 2 m, with one reaching 5.8 m. This storm activity was similar to that during other recent years, and sufficient for analysis of storm-generated currents as they affect bottom sediment resuspension.</p> <p>The moored instrumentation at the PDS yielded nearly complete records of near-bottom currents, water temperature, pressure, and relative turbidity over the period from late February to mid-May 1996. Hourly averaged near-bottom current speeds during the measurement period ranged from 0 to approximately 0.4 knots ($\sim 20 \text{ cm s}^{-1}$), with the majority of the variability occurring at periods of approximately 12 hr in association with the semi-diurnal tide. Tidal harmonic analysis of the current velocity data revealed that the amplitude of the M_2 semi-diurnal tidal current is weak (approximately 3 cm s^{-1}), but significantly stronger than all other tidal constituents.</p> <p>Time-series measurements of near-bottom turbidity during the 78-day measurement period were acquired using optical sensors at levels of 33 and 81 cm above the seafloor. Detailed analysis of the near-bottom current data during the nine storms revealed that high-frequency oscillatory currents could be induced by large-amplitude surface waves, resulting in relatively high bottom stress and sediment resuspension as confirmed by elevated near-bottom turbidity levels. The field observations of near-bottom turbidity were useful for documenting that sediment resuspension had occurred during a subset of the storms, but the measurement program was not designed to quantify the depth of erosion nor the volume (per unit area) of sediment that had been eroded during the storms. Furthermore, additional analysis and numerical modeling of the data to determine the complex interactions between wave height, period, and duration, the speed and direction of background currents, and the availability of fine-grained bottom sediments on sediment resuspension at the PDS was beyond the scope of this project.</p>				
14. SUBJECT TERMS current measurement, turbidity, suspended solids, thermocline, pycnocline and wave dynamics			15. NUMBER OF PAGE 62	
			16. PRICE CODE	
17. SECURITY CLASSIFICATION OF REPORT Unclassified	18. SECURITY CLASSIFICATION OF THIS PAGE	19. SECURITY CLASSIFICATION OF ABSTRACT	20. LIMITATION OF ABSTRACT	

**OCEANOGRAPHIC MEASUREMENTS
AT THE PORTLAND DISPOSAL SITE
DURING SPRING OF 1996**

CONTRIBUTION #121

MAY 1998

Report No.
SAIC 388

Submitted to:
Regulatory Branch
New England District
U.S. Army Corps of Engineers
696 Virginia Road
Concord, MA 01742-2751

Prepared by:
Scott E. McDowell
Stephen D. Pace

Submitted by:
Science Applications International Corporation
Admiral's Gate
221 Third Street
Newport, RI 02840
(401) 847-4210



**US Army Corps
of Engineers**

New England District

TABLE OF CONTENTS

	Page
LIST OF TABLES.....	iv
LIST OF FIGURES	v
EXECUTIVE SUMMARY	viii
1.0 INTRODUCTION	1
1.1 Background	1
1.2 Site Characteristics	1
1.3 Project Objectives	3
1.4 Report Contents	5
2.0 DESCRIPTION OF FIELD MEASUREMENT PROGRAM.....	6
2.1 Field Operations	6
2.1.1 Field Schedule and Logistics	6
2.1.2 Selection of Deployment Site for Moored Instrumentation.....	6
2.1.3 Deployment and Recovery of Moored Instrumentation	8
2.1.4 Water Column Profile Measurements.....	8
2.1.5 Sediment Grab Samples	9
2.2 Instrumentation and Data Acquisition Procedures.....	9
2.2.1 Bottom-Mounted Instrument Array.....	9
2.2.2 Near-Bottom Current Velocity and Turbidity Sensors	9
2.2.3 Post-Survey Laboratory Calibration of Turbidity Sensors.....	11
2.2.4 Water Column Profiling Instrumentation.....	13
2.2.5 Meteorological Observations from NOAA Buoy 44007	13
3.0 OCEANOGRAPHIC ANALYSES.....	14
3.1 Water Column Characteristics	14
3.2 Surface Wave Climatology.....	20
3.2.1 Time Series of Meteorological Observations	20
3.2.2 Annual Wave Statistics	24
3.2.3 Seasonal Wave Statistics	27
3.2.4 Duration of Storm Waves.....	28
3.2.5 Meteorological Conditions during Spring of 1996.....	28
3.3 Assessment of Currents and Physical Processes	30
3.3.1 Analysis of Near-Bottom Currents	30
3.3.2 Analysis of Near-Bottom Turbidity	39
3.3.3 Analysis of Near-Bottom Currents and Turbidity during Storm Events.....	41

TABLE OF CONTENTS (continued)

	Page
4.0 SUMMARY OF MONITORING RESULTS	58
5.0 REFERENCES	61
INDEX	
APPENDICES	

LIST OF TABLES

	Page
Table 3-1. Annual Statistics of Significant Wave Heights for the Period from January 1993 through May 1996 as Observed by NOAA Buoy 44007. Upper: Percent Occurrence of Hourly Observations within Specific Wave Height Ranges. Middle: Duration (hours) of Significant Wave Heights above Specific Wave Heights. Lower: Maximum Significant Wave Height.....	26
Table 3-2. Seasonal Wave Statistics for the Period from January 1993 through May 1996 as Observed by NOAA Buoy 44007.....	28
Table 3-3. Duration Intervals and Significant Wave Heights of Major Storms during the Period from January 1993 through May 1996 as Observed by NOAA Buoy 44007.....	30
Table 3-4. Summary of Maximum Wave Heights, Peak Wave Periods, Duration of Wave Heights Greater than 3 m, and Maximum of the Burst-Averaged Standard Deviation in Near-Bottom Current Speeds during Nine Storm Events during the Period from February 27 to May 14, 1996.....	43
Table 3-5. Summary of Maximum Wave Heights, Maximum of the Burst-Averaged Standard Deviation in Near-Bottom Current Speeds, Background (Pre-Storm) Concentration of Total Suspended Solids (TSS), Maximum TSS during Storms, and Duration of Elevated TSS during Nine Storm Events during the Period from February 27 to May 14, 1996	55

LIST OF FIGURES

	Page
Figure 1-1.	Location of Portland Disposal Site and NOAA buoy 44007 in the Gulf of Maine east of Cape Elizabeth..... 2
Figure 1-2.	Bathymetric chart (in meters relative to MLLW) of the southern half of the Portland Disposal Site as determined from a survey conducted in February 1996 by SAIC..... 4
Figure 2-1.	Locations of moored array deployments within the southwestern corner of the Portland Disposal Site during spring of 1996 7
Figure 2-2.	Schematic diagram of the moored instrument array used to acquire near-bottom measurements of horizontal currents, water temperature, and relative turbidity (at heights of 33 and 81 cm above the seafloor) within the Portland Disposal Site during spring of 1996 10
Figure 2-3.	Plot illustrating the results of the laboratory calibration to determine the correlation between relative turbidity (in NTUs) measured by the Seapoint turbidity sensor versus suspended solids concentrations (in $\text{mg}\cdot\text{l}^{-1}$) determined by laboratory procedures 12
Figure 3-1a.	Vertical profiles of temperature, salinity, and density ($\sigma\text{-t}$) acquired at the Portland Disposal Site on February 27, 1996 15
Figure 3-1b.	Vertical profiles of temperature, salinity, and density ($\sigma\text{-t}$) acquired at the Portland Disposal Site on April 22, 1996..... 16
Figure 3-1c.	Vertical profiles of temperature, salinity, and density ($\sigma\text{-t}$) acquired at the Portland Disposal Site on May 14, 1996..... 18
Figure 3-2.	Temperature/salinity characteristics of the three vertical profiles (see Figures 3-1a through c) acquired at the Portland Disposal Site during spring of 1996..... 19
Figure 3-3a.	Time series plot of meteorological and wave data from NOAA buoy 44007 during the period from January 1993 to January 1994 21

LIST OF FIGURES (continued)

	Page
Figure 3-3b. Time series plot of meteorological and wave data from NOAA buoy 44007 during the period from February 1994 to January 1995	22
Figure 3-3c. Time series plot of meteorological and wave data from NOAA buoy 44007 during the period from January 1995 to January 1996	23
Figure 3-3d. Time series plot of meteorological and wave data from NOAA buoy 44007 during the period from January through May 1996.....	25
Figure 3-4. Time series plot of meteorological and wave data from NOAA buoy 44007 during the period from March through May 1996, corresponding with the period of the oceanographic measurement program	29
Figure 3-5. Time series plot of near-bottom data acquired during the 3-month measurement period.....	32
Figure 3-6. Time series plot of bottom pressure (upper tier), near-bottom water temperature (middle tier), and near-bottom current vectors (lower tier) during the 3-month measurement period.....	34
Figure 3-7. Tidal current ellipses for the M2 semidiurnal tidal constituent for the first (left) and third (right) deployment periods	37
Figure 3-8. Time series plot of hourly observed currents (after the mean had been removed), predicted tidal currents, and residual (observed minus predicted) currents for the first and third deployment periods	38
Figure 3-9. Time series plot of near-bottom current data and surface wave data during the 3-month measurement period.....	40
Figure 3-10. Time series plot of data from the 3-month measurement period.....	42
Figure 3-11a. Time series plot of surface wave and near-bottom current and turbidity data during storm 1	44

LIST OF FIGURES (continued)

	Page
Figure 3-11b. Time series plot of surface wave and near-bottom current and turbidity data during storm 2	45
Figure 3-11c. Time series plot of surface wave and near-bottom current and turbidity data during storm 3	46
Figure 3-11d. Time series plot of surface wave and near-bottom current and turbidity data during storm 4	47
Figure 3-11e. Time series plot of surface wave and near-bottom current and turbidity data during storms 5 and 6.....	48
Figure 3-11f. Time series plot of surface wave and near-bottom current and turbidity data during storm 6	49
Figure 3-11g. Time series plot of surface wave and near-bottom current and turbidity data during storm 7	50
Figure 3-11h. Time series plot of surface wave and near-bottom current and turbidity data during storm 8	51
Figure 3-11i. Time series plot of surface wave and near-bottom current and turbidity data during storm 9	52
Figure 3-12. Plot illustrating the relationship between maximum significant wave height and the maximum standard deviation in near-bottom current speed for the nine storm events presented in Table 3-4.....	56

EXECUTIVE SUMMARY

Under the Disposal Area Monitoring System (DAMOS) Program for the U.S. Army Corps of Engineers, New England Division, Science Applications International Corporation (SAIC) conducted an Oceanographic Measurement Program at the Portland Disposal Site (PDS) located 13 km east of Cape Elizabeth in the Gulf of Maine. A single instrumented tripod was deployed from February 27 to May 14, 1996, in order to acquire site-specific data on tides and near-bottom currents, water temperature, and turbidity. The tripod was deployed in the southwest corner of the PDS, in a region of relatively rough topography having a water depth of approximately 60 m. Overall, the 78-day measurement program provided excellent data from which to characterize near-bottom currents and turbidity, and evaluate the physical processes governing bottom sediment resuspension within the PDS.

Vertical profiles of temperature, salinity, and density were acquired at a single location in the PDS during February, April, and May 1996, respectively. The February profile revealed a water column that was very weakly stratified, as is typical for the coastal Gulf of Maine in winter. Water property characteristics during late April and mid-May illustrated that relatively fresh and warm water had been introduced to the surface layer, presumably as a result of river discharge. Beneath a moderate thermocline and pycnocline, water properties were nearly constant throughout the lower half of the water column during late spring. With regard to the vertical density stratification, it is apparent that the entire water column to a depth of 60 m is very weakly stratified throughout winter and early spring, whereas the introduction of relatively fresh/warm waters at the surface during mid-spring causes considerable stratification that may tend to decouple horizontal currents and other transport processes within a two-layer water column.

Time series observations of winds, waves, atmospheric pressure, and surface water temperatures were acquired from NOAA buoy 44007, located 6 km southwest of the PDS, to assess the seasonal and inter-annual variability in meteorological conditions from 1993 through 1995, as well as meteorological conditions during the 1996 measurement program. Analysis of the annual wave statistics revealed that wave characteristics were very similar for the 3.4 years of wave records. Significant wave heights less than 2 m occurred from 90 to 95% of the time during each year. The maximum significant wave height observed in each of the four measurement years ranged from 5.6 to 7.3 m. Overall, wave characteristics during the first half of 1996 were typical of other recent years at this location.

Analysis of the seasonal variability in wave conditions at the PDS revealed that mean significant wave heights were 1.2 m in winter (December through February) and

EXECUTIVE SUMMARY (continued)

approximately 1 m or less for the other three seasons. Maximum significant wave heights were roughly 3 m in summer, compared to 6 m in winter, and 7 m in spring and fall.

Quantitative analysis of storm waves revealed 72 events during the 3.4-year analysis period that had significant wave heights between 3 and 4 m; average durations for these wave events were only 6 to 8 hrs. Wave heights in the range of 5 to 6 m were observed only 22 times with average durations of less than 3 hrs.

The wave records from March through May 1996 exhibited nine storm events attaining significant wave heights greater than 2 m, with one reaching 5.8 m. This storm activity was similar to that during other recent years, and sufficient for analysis of storm-generated currents as they affect bottom sediment resuspension.

The three consecutive deployments of moored instrumentation at the PDS yielded nearly complete records of near-bottom currents, water temperature, pressure, and relative turbidity over the period from late February to mid-May 1996. Hourly averaged near-bottom current speeds during the measurement period ranged from 0 to approximately 0.4 knots ($\sim 20 \text{ cm}\cdot\text{s}^{-1}$), with the majority of the variability occurring at periods of approximately 12 hr in association with the semi-diurnal tide. Tidal harmonic analysis of the current velocity data revealed that the amplitude of the M_2 semi-diurnal tidal current is weak (approximately $3 \text{ cm}\cdot\text{s}^{-1}$), but significantly stronger than all other tidal constituents.

The mean current speed for each of the three deployments was very consistent ($7.0 \pm 0.4 \text{ cm}\cdot\text{s}^{-1}$), but the mean direction varied greatly among the deployments, presumably due to rough topography (e.g., boulders and rock ledges) in close proximity to the moored instrumentation. Analysis of residual currents (after the mean current and the tidal currents had been removed from the observed records) revealed that storms had almost no effect on hourly averaged near-bottom currents at the PDS.

Time-series measurements of near-bottom turbidity during the 78-day measurement period were acquired using optical sensors at levels of 33 and 81 cm above the seafloor. Both sensors provided excellent quality data (with no appreciable biofouling) such that small turbidity fluctuations above a consistently low background level could be distinguished. Near-bottom turbidity data acquired during the nine storm events having significant wave heights greater than 2 m (from late February through mid-May 1996) revealed that substantial quantities of ambient bottom sediments were resuspended during two storms having maximum significant wave heights in excess of 3 m. However, sediment resuspension was minimal or nonexistent for seven other storms having maximum

EXECUTIVE SUMMARY (continued)

significant wave heights in the range of 2 to 4 m. This result illustrated that bottom sediment resuspension at the PDS was not simply a function of surface wave height.

Detailed analysis of the near-bottom current data during the nine storms revealed that high-frequency oscillatory currents could be induced by large-amplitude surface waves, resulting in relatively high bottom stress and sediment resuspension as confirmed by elevated near-bottom turbidity levels. The field observations of near-bottom turbidity were useful for documenting that sediment resuspension had occurred during a subset of the storms, but the measurement program was not designed to quantify the depth of erosion nor the volume (per unit area) of sediment that had been eroded during the storms. Furthermore, additional analysis and numerical modeling of the data to determine the complex interactions between wave height, period, and duration, the speed and direction of background currents, and the availability of fine-grained bottom sediments on sediment resuspension at the PDS was beyond the scope of this project.

1.0 INTRODUCTION

1.1 Background

Portland Harbor is being considered for maintenance dredging to remove the natural accumulation of sediments from its channels and berths. The use of capping to isolate dredged sediments may be needed in order to accomplish this or other projects, thus the efficacy of capping at the Portland Disposal Site (PDS) needed to be demonstrated by the New England Division (NED) of the U.S. Army Corps of Engineers. Capping has been successfully used as a remediation technique at PDS (Wiley 1996) and at dredged material disposal sites throughout Long Island Sound for nearly 20 years (SAIC 1995a). However, approval for routine use of this technique at the greater depths of PDS would be facilitated if a successful demonstration could be conducted.

As a component of the Disposal Area Monitoring System (DAMOS), NED managed two investigations at PDS during the Fall and Winter of 1995-1996 to demonstrate that disposed dredged material could effectively be capped and isolated from the environment by a layer of clean sediment. The two investigations, both conducted by Science Applications International Corporation (SAIC), were the Capping Demonstration Study (SAIC 1995b) and the Oceanographic Measurement Program. The objective of the Capping Demonstration Study was to use uncontaminated sediments dredged from the Royal River to create both a disposal mound and a cap, each composed of different sediment types. If the cap material was placed over the mound successfully, without mixing of the two sediment types, cap construction techniques would thus be demonstrated in the relatively deep waters of PDS. In addition, the ability of the cap material to resist resuspension and horizontal transport after placement also needed to be demonstrated at the disposal site. To test this hypothesis, an Oceanographic Measurement Program was designed and implemented by SAIC to acquire site-specific data on near-bottom currents and resuspension of natural sediments at PDS to demonstrate cap stability through winter/spring storms. This report presents a summary of the results obtained from this measurement program.

1.2 Site Characteristics

PDS is located approximately 13 km east of Cape Elizabeth in the western Gulf of Maine (Figure 1-1). Originally used for dredged material disposal by the War Department from 1943 to 1946, and by NED in 1979, PDS was designated by Region I EPA on October 16, 1987, as an Ocean Disposal Site for harbor dredging projects throughout the

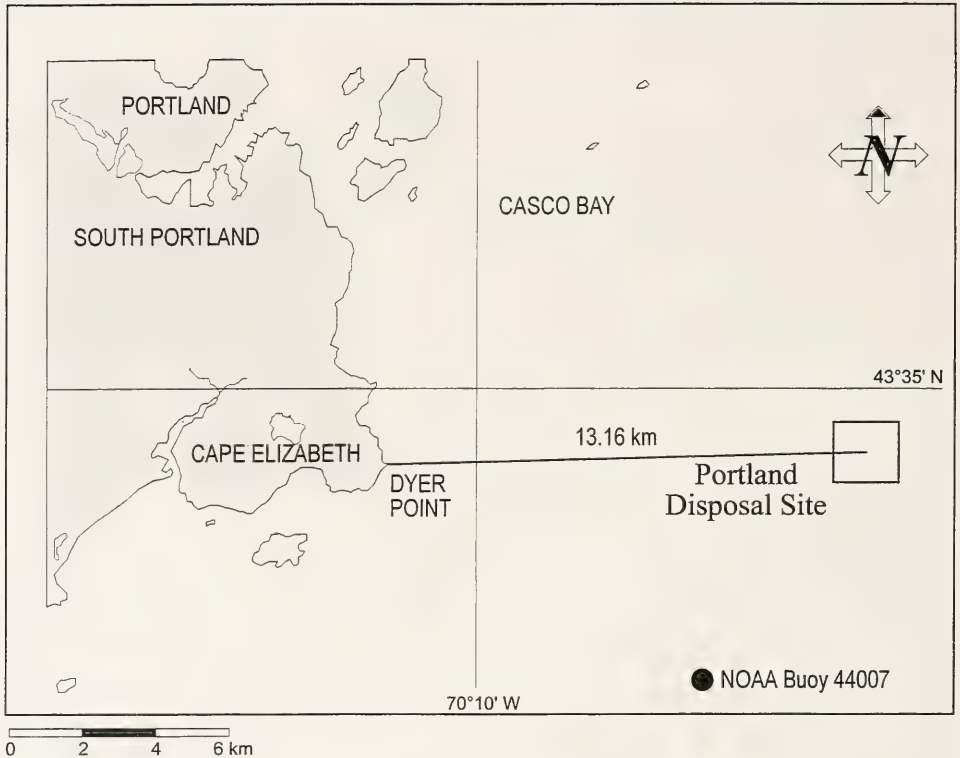


Figure 1-1. Location of Portland Disposal Site and NOAA buoy 44007 in the Gulf of Maine east of Cape Elizabeth

Portland, Maine, area (EPA 1987). The majority of recent disposal activities have been restricted to the northern half of the site, at continually moored marker buoys. The southeastern corner of PDS (Figure 1-2) has been selected as the site for disposal of material from the Royal River under the Capping Demonstration project.

Water depths within the southern half of PDS range from roughly 40 to 70 m (Figure 1-2) as determined from recent bathymetric surveys conducted by SAIC. For the Oceanographic Measurement Program, instrumentation was moored in the southwestern corner of PDS to minimize potential short-term effects of dredged material disposal on near-bottom turbidity.

PDS is susceptible to storms because of unlimited fetch toward the south and southeast. Large waves during winter storms are expected to generate substantial currents which may reach the seafloor within the site and hence cause resuspension of fine-grained material, whether ambient or derived from dredged material.

PDS is characterized by rocky, irregular relief composed of a complex network of bedrock outcrops, steep ridges caused by glacial scour, and small topographic depressions containing natural sedimentary deposits of gravel, sand, silt, and clay (Morris 1996).

The temporal variability of water properties and near-bottom currents within PDS is poorly understood, as there have been few site-specific measurements. The only known current measurements were acquired in August and September of 1979 using an instrument situated 1.5 m above the seafloor (NUSC 1979). The observations showed that near-bottom currents are generally weak (less than 1/3 knot), but because the instrument only acquired current measurements at 2-minute intervals, the data were insufficient for assessment of high-frequency processes (i.e., surface wave effects) that may affect bottom sediment resuspension. Current measurements at other locations within the western Gulf of Maine indicate that currents are generally weak (less than 1/2 knot) and dominated by the semi-diurnal tide. Likewise, no time series of meteorological conditions (e.g., wind and wave characteristics) have been acquired within the site, but long-term, near-continuous data can be obtained from NOAA buoy 44007 located 6 km southwest of PDS (see Figure 1-1).

1.3 Project Objectives

The primary objective of the Oceanographic Measurement Program was to monitor and evaluate the physical processes that may affect the long-term physical stability of capped disposal mounds at PDS. Moored instrumentation was deployed in the southwestern corner of the site from late February to early May 1996 in order to acquire

Portland Disposal Site Bathymetry (m)

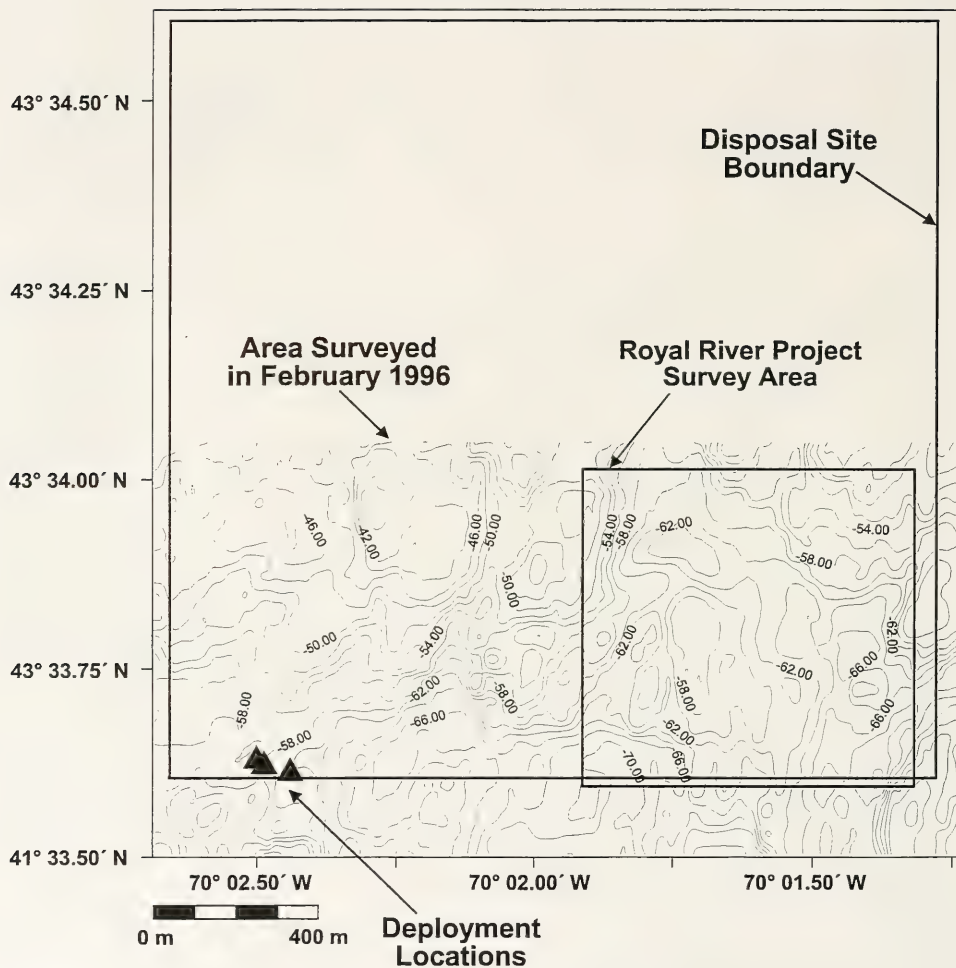


Figure 1-2. Bathymetric chart (in meters relative to MLLW) of the southern half of the Portland Disposal Site as determined from a survey conducted in February 1996 by SAIC. The locations of the spring 1996 current measurements in the southwestern corner of the site are indicated, as well as the area delineated for the Royal River Disposal Project.

time-series records of near-bottom currents, water temperature, and relative turbidity during winter storm events that may induce bottom sediment resuspension. The measurement data were analyzed to determine whether low-frequency, tidal, and/or storm-induced currents have sufficient magnitude to erode natural bottom sediments. The results also represent valuable data for later use in validating hindcast and forecast models of the erosion of capped mounds at PDS under a variety of storm conditions.

1.4 Report Contents

Following this Introduction, Section 2 presents a description of the field measurement program conducted at PDS, including field operations, instrumentation, and procedures for data acquisition and processing. Section 3 presents the results of the measurement program, including water column characteristics, surface wave climatology, near-bottom currents and turbidity, as well as a discussion of the processes affecting bottom sediment resuspension. A summary of the results is presented in Section 4. Section 5 presents pertinent references. Two Appendices present tabular results on wave climatology in the vicinity of PDS.

2.0 DESCRIPTION OF FIELD MEASUREMENT PROGRAM

2.1 Field Operations

2.1.1 Field Schedule and Logistics

Deployment, servicing, and final recovery of the moored instrumentation at the Portland Disposal Site (PDS) were accomplished during four field operations. The initial trip, conducted on February 27, 1996, entailed selection of a suitable site for the oceanographic measurements and deployment of the instrument array. During the second and third trips, conducted on April 6 and April 23, respectively, the instrument array was recovered, serviced to replace batteries and acquire data from the internally recording instrumentation, and redeployed. The final trip was conducted on May 14 to recover the array and acquire data from the final deployment period.

The timing and executions of field operations were highly dependent on winter weather conditions, and two vessels were employed depending on availability. The first two deployment/servicing cruises were conducted with assistance from the able crew of the University of New Hampshire's research vessel *Gulf Challenger*, based at Portsmouth, NH. The final two cruises were accomplished using the commercial fishing vessel *Susan & Caitlyn*, from a home port in Portland, ME.

2.1.2 Selection of Deployment Site for Moored Instrumentation

During the February 27, 1996 field trip to the proposed deployment site, a brief high-resolution bathymetric survey was conducted to aid in selection of the optimum location for deployment of the moored array. This survey revealed a small, relatively level area in the southwestern quadrant of the site that appeared suitable for deployment of equipment (Figure 2-1). The target deployment site, located at 43°33.63' N, 70°02.49' W at a water depth of 58 m below mean lower low water (MLLW), was approximately 1.5 km southwest of the location where dredged material was disposed at various times during the spring 1996 measurement program.

Although the bathymetric contours presented in Figure 2-1 illustrate smoothly varying topography in the vicinity of the proposed mooring site, the actual topography was extremely rough (see below), which is a reminder that considerable spatial averaging of bathymetric soundings is performed in the process of generating a gridded depth matrix from which bathymetric contour plots are created.

Portland Disposal Site Moored Array Deployment Locations

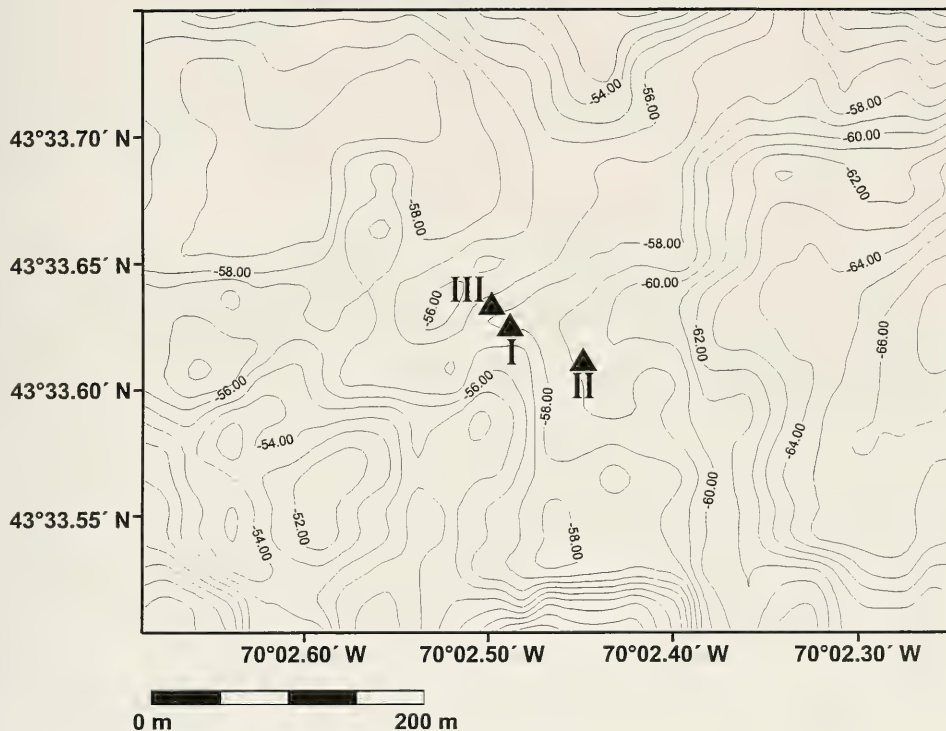


Figure 2-1. Locations of moored array deployments within the southwestern corner of the Portland Disposal Site during spring of 1996. Bathymetric results (in meters relative to MLLW) were derived from a survey in February 1996.

In conjunction with the larger bathymetric survey conducted in February 1996 (see Figure 1-2), SAIC also acquired analog sidescan sonar data along east-west lanes spaced 150 m apart across the southern half of PDS. Analysis of the analog sidescan records acquired in close proximity to the target deployment location revealed that the seafloor topography was very rough, with large boulders and features ranging from a few meters in height to large rock ledges extending for distances of hundreds of meters. Nevertheless, this location was chosen for the deployment of the moored array as it was the most level region within the southwestern corner of PDS. As described in further detail below, the final deployment site was characterized by silty sand and numerous boulders, and bordered on the northeast by a large rock ledge within 100 m of the deployment site.

2.1.3 Deployment and Recovery of Moored Instrumentation

For all cruises, SAIC provided navigation equipment for vessel positioning during deployment/recovery operations. Precision positioning data were acquired using a Differential Global Positioning System (DGPS) receiver interfaced to SAIC's Portable Integrated Navigation Survey System (PINSS) software. The PINSS provided helmsman displays to facilitate continuous, real-time assessment of vessel position and drift in relationship to target locations.

Instrument deployments were conducted after the vessel had reached the target location and determined the speed and direction of vessel drift due to winds and currents. Next, the instrument array was lowered by a winch wire to approximately 2 m above the seafloor while the vessel position was checked versus the target location. Release of the instrument array was accomplished using either a release hook or a secondary acoustic release attached to the winch wire. Both the vessel position and the exact time of release were recorded by the PINSS.

For array recovery operations, the acoustic release on the array was interrogated, using an acoustic deckbox and transducer, after the vessel had been positioned in close proximity to the array deployment location. Following interrogation, the array released flotation that was attached to a line canister, allowing a small buoy to reach the sea surface. The buoy's tether was used to raise the array from the seafloor and place it on the deck of the vessel. The internally recording instrumentation was subsequently serviced and electronic data were downloaded using a portable computer.

2.1.4 Water Column Profile Measurements

A single vertical profile of temperature, salinity (conductivity), and density was acquired at the site of the moored instrumentation during the first, third, and fourth cruises

to PDS. These data were used to assess water column structure and facilitate comparison with the near-bottom water temperature data acquired by the moored instrument array.

2.1.5 Sediment Grab Samples

During the final instrument recovery cruise on May 14, 1996, bottom sediment samples were collected using a grab sampler and returned to SAIC's laboratory for visual assessment of sediment characteristics at the site of the moored instrumentation. Visual analysis showed that the sediments were comprised of fractions of small rocks, gravel, sand, silt, and clay. The predominant fractions were a sand, silt, and clay. The water content of this sediment was approximately 129%, which was determined using the formula:

$$\text{water content} = \left(\frac{\text{weight of wet sediment sample}}{\text{weight of dry sediment sample}} \right) \times 100$$

As described below, the sediment samples were used for post-cruise laboratory calibration of the optical turbidity sensors mounted on the instrument array.

2.2 Instrumentation and Data Acquisition Procedures

2.2.1 Bottom-Mounted Instrument Array

The instrument array was composed of an aluminum tripod frame, an electro-magnetic current meter, two turbidity sensors and a water temperature sensor interfaced to a datalogger, and an acoustic recovery system (Figure 2-2). The tripod was constructed of 2.5-in diameter Schedule 80 aluminum round stock, and 0.5-in aluminum flat stock welded and bolted together to facilitate deployments from small vessels-of-opportunity. Because of concern about the reliability of data from the electromagnetic current meter in close proximity to the tripod hardware, no zinc anodes were attached to the tripod. As an added precaution, Delryn material was placed between all tripod elements and stainless steel bolts were used to join the tripod elements.

2.2.2 Near-Bottom Current Velocity and Turbidity Sensors

An InterOcean S-4DW internally recording, electro-magnetic current meter was used to acquire current velocity data from a height of 46 cm above the seafloor (Figure 2-2). The S-4DW was mounted beneath the apex of the tripod to minimize flow turbulence in close proximity to the legs of the tripod. With regard to data recording capabilities, the S-4DW was equipped with 1 megabyte of memory and programmed to record vector-averaged data in a "burst sampling" mode. During each burst, current vector data were sampled at 0.5 Hz intervals over a 1-minute period, yielding 30 current measurements per

Bottom-Mounted Instrument Array

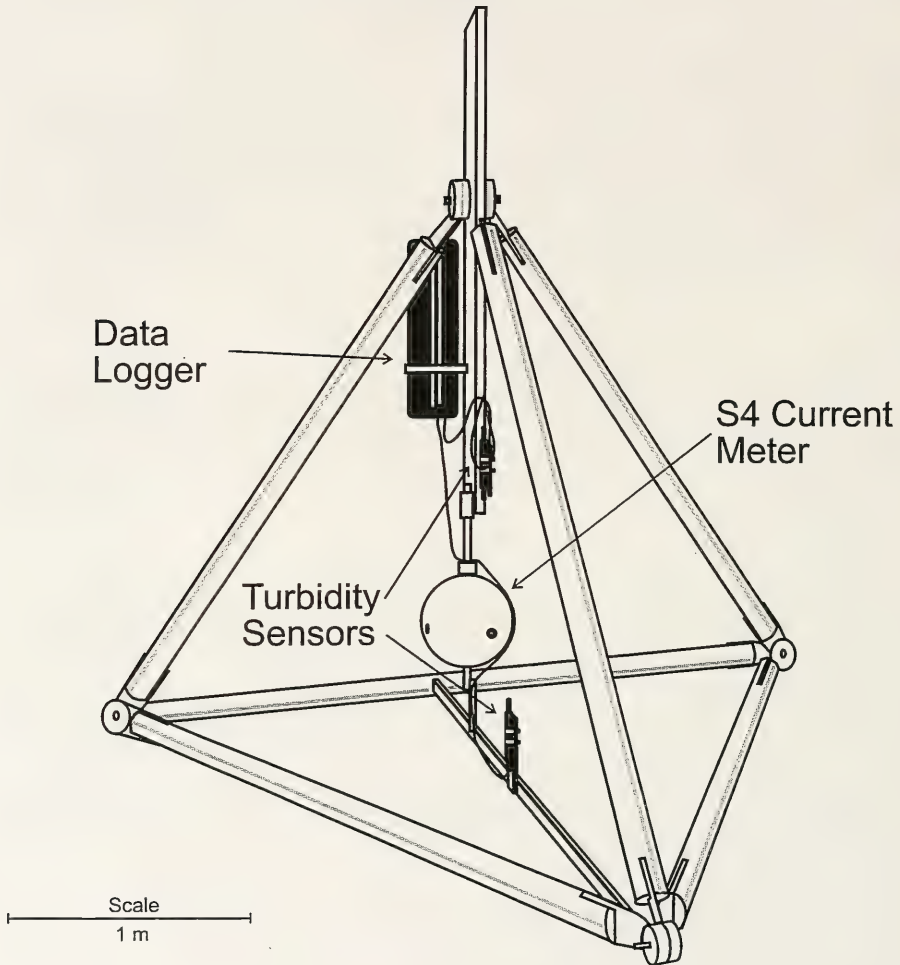


Figure 2-2. Schematic diagram of the moored instrument array used to acquire near-bottom measurements of horizontal currents, water temperature, and relative turbidity (at heights of 33 and 81 cm above the seafloor) within the Portland Disposal Site during spring of 1996

burst; bursts were acquired at 10-minute intervals over the entire deployment period. In addition, a single pressure measurement was acquired during each burst in order to assess water level (tides).

Hourly measurements of near-bottom turbidity were acquired using two optical turbidity sensors manufactured by Seapoint Sensors, Inc. Analog data from the turbidity sensors, located at heights of 33 and 81 cm above the seafloor (Figure 2-2), were recorded by a programmable Model R2 data logger manufactured by Dryden Instrumentation Inc. In addition, near-bottom water temperature data were acquired and recorded by the logger at hourly intervals.

For the overall measurement program, 100% of the current velocity, bottom pressure, turbidity, and water temperature data were recovered over the 78-day deployment period, except during two brief (less than 12-hour) servicing events.

2.2.3 Post-Survey Laboratory Calibration of Turbidity Sensors

Following the field measurement program, the relative turbidity sensors were calibrated using standard laboratory procedures as recommended by the manufacturer (Seapoint Sensors, Inc.) Sediment samples from the deployment site (composed predominantly of silts and clays) were homogenized and wet sieved through 63-micron mesh to remove gravel and sand, as the primary objective of the field program was to assess whether currents were sufficient to resuspend fine-grained sediment residing on the seafloor. The supernatant was dried and then weighed to determine the mass of the sediment sample. A 1-gram subsample of fine sediment was then hydrated and serially diluted with filtered seawater from Narragansett Bay to achieve a suite of representative concentrations of suspended solids.

One of the turbidity sensors was interfaced to the data logger used during the field program and immersed in the slurry of suspended solids to acquire relative turbidity measurements (in Nephelometry Turbidity Units [NTUs]) for comparison with the known suspended solids concentration. Intercomparison data were acquired over a broad range of suspended solids concentrations; results in the range from 0 to 32 $\text{mg}\cdot\text{l}^{-1}$ are presented in Figure 2-3. As indicated in the figure, a linear calibration was evident over the range of suspended solids concentrations measured in the field (see Section 3). This relationship was used to convert the field measurements of relative turbidity into units of $\text{mg}\cdot\text{l}^{-1}$ suspended solids concentration.

It is important to note, however, that the laboratory calibration of the turbidity sensor is prone to some uncertainty at very low suspended solids concentrations (e.g., less

Laboratory Calibration using Portland Sediments

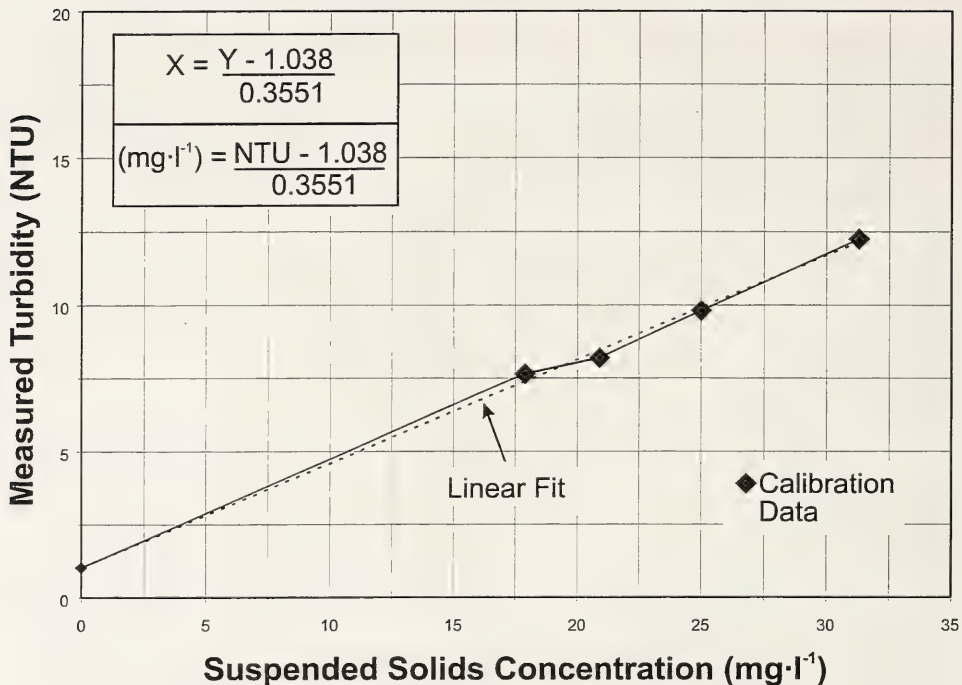


Figure 2-3. Plot illustrating the results of the laboratory calibration to determine the correlation between relative turbidity (in NTUs) measured by the Seapoint turbidity sensor versus suspended solids concentrations (in mg·l⁻¹) determined by laboratory procedures. A linear relationship was used to convert from NTUs to mg·l⁻¹ for all monitoring data.

than $5 \text{ mg}\cdot\text{l}^{-1}$). One potential source of this low-end variability is associated with the characteristics of the measurement medium. For example, the laboratory calibration used filtered seawater that may have had significantly different concentrations and particle size characteristics of any remaining suspended solids compared to the "background" conditions of the near-bottom water at the Portland measurement site. Consequently, when the relative turbidity data from the Portland field site were converted to suspended solids concentrations using the laboratory calibration equation, some of the low-end values resulted in concentrations less than zero (e.g., see Figures 3-11a and 3-11e). Because this low-end uncertainty had no adverse effect on the analyses or interpretations of this study, no attempt was made to modify the turbidity calibration equation.

2.2.4 Water Column Profiling Instrumentation

Water column profile measurements were acquired using a SeaCat Conductivity-Temperature-Depth (CTD) profiling instrument manufactured by Sea-Bird Electronics, Inc. to characterize water properties at the site of the moored instrument array. On three of the four trips to the site, the SeaCat was lowered to the seafloor to acquire data from near the surface to within a few meters of the seafloor. During profiling operations, the SeaCat sampled conductivity, temperature, and pressure (instrument depth) at 1-sec intervals, which was sufficient to acquire data at approximately 10-cm intervals through the vertical profile. Following the survey, the CTD data were downloaded, edited, and used to generate graphic data products depicting the vertical structure in water properties at the measurement site.

2.2.5 Meteorological Observations from NOAA Buoy 44007

NOAA buoy 44007, located 6 km southwest of the moored instrument site (at $43^{\circ}31.48'\text{N}$ and $70^{\circ}05.24'\text{W}$), provided meteorological data throughout the spring 1996 measurement program. The data that were most applicable to the present program were wind speed and direction, atmospheric pressure, surface water temperature, significant wave height, and peak wave period (the period of the wave having the peak spectral density). Buoy data were acquired electronically from NOAA for the period from January 1993 through May 1996 and archived with the moored current data from the Portland Disposal Site.

In general, the NOAA buoy provided good-quality data for all parameters and the 3.4 years of data were adequate to develop annual and seasonal statistics for all meteorological parameters of concern.

3.0 OCEANOGRAPHIC ANALYSES

3.1 Water Column Characteristics

Water mass characteristics above 200 m depth in the Gulf of Maine are controlled mainly by seasonal changes in the surface heat transfer processes, river runoff, and influx of relatively cold waters from the northeast, originating on the Scotian shelf (Hopkins and Garfield 1977). During winter, storms induce considerable vertical mixing and near-elimination of the density stratification in the water column, thereby allowing the relatively fresh, near-surface waters to mix with the more saline deep water within the Gulf of Maine. The resulting cold water mass, which is formed only in winter, has been named Gulf of Maine Intermediate Water (MIW) by Hopkins and Garfield (1977). In support of this hypothesized winter process, Brown and Beardsley (1978) have demonstrated that cold offshore winds during winter are effective at cooling the near-surface waters and causing intermittent overturning of the upper water column, which, in turn, leads to formation of MIW.

With the onset of spring along the western Gulf of Maine, river runoff contributes a significant volume of much fresher (and somewhat warmer) water, resulting in significant density stratification in the upper 20 m of the water column. This stratification continues to intensify during summer and early fall due to continual warming of the surface waters, although near-surface salinities remain relatively constant.

As described in Section 2.0, vertical profiles of temperature, salinity, and density (σ_t) were acquired at a single location in the Portland Disposal Site (PDS) during three events associated with deployment, servicing, and recovery of the moored instrumentation: February 27, April 22, and May 14, 1996, respectively. Vertical profiles of all three variables over the depth range from 3 to 58 m (2 m above the seafloor) during February are presented in Figure 3-1a. The February profiles of salinity and density indicate an isohaline/isopycnal layer above 6 m depth, and gradually increasing salinity and density over the depth range from 9 m to the seafloor. Salinities ranged from roughly 31.0 to 32.4 ppt over the full extent of the water column. Water temperature in February exhibited more vertical structure than salinity: temperatures were relatively constant (near 3°C) over the upper 20 m of the water column, but beneath that level, temperatures increased monotonically to a maximum of roughly 4.8°C near the bottom. Overall, Figure 3-1a illustrates a water column that is very weakly stratified, as is typical for the coastal region of the Gulf of Maine during later winter (Brown and Beardsley 1978).

Water property characteristics during late April (Figure 3-1b) illustrate that relatively fresh/warm waters had been introduced to the near-surface layer as a result of river

Water Column Profiles Portland Disposal Site February 27, 1996

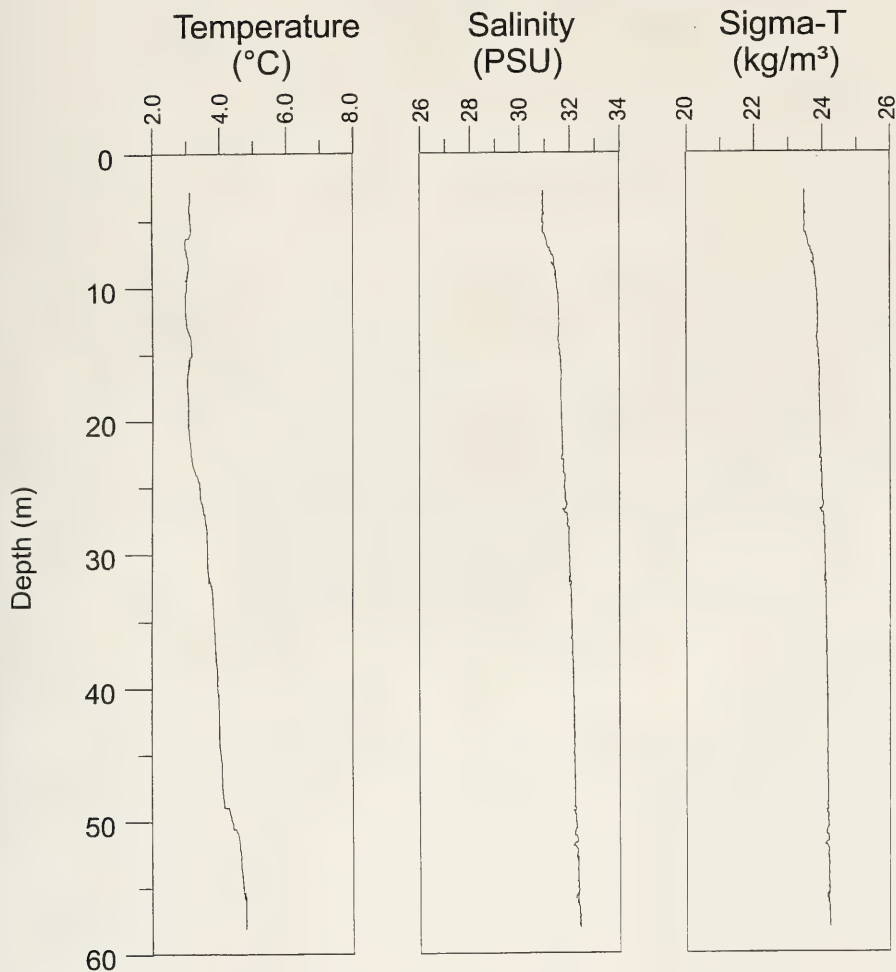


Figure 3-1a. Vertical profiles of temperature, salinity, and density (sigma-t) acquired at the Portland Disposal Site on February 27, 1996. Water depth at the measurement site was 60 m.

Water Column Profiles Portland Disposal Site April 22, 1996

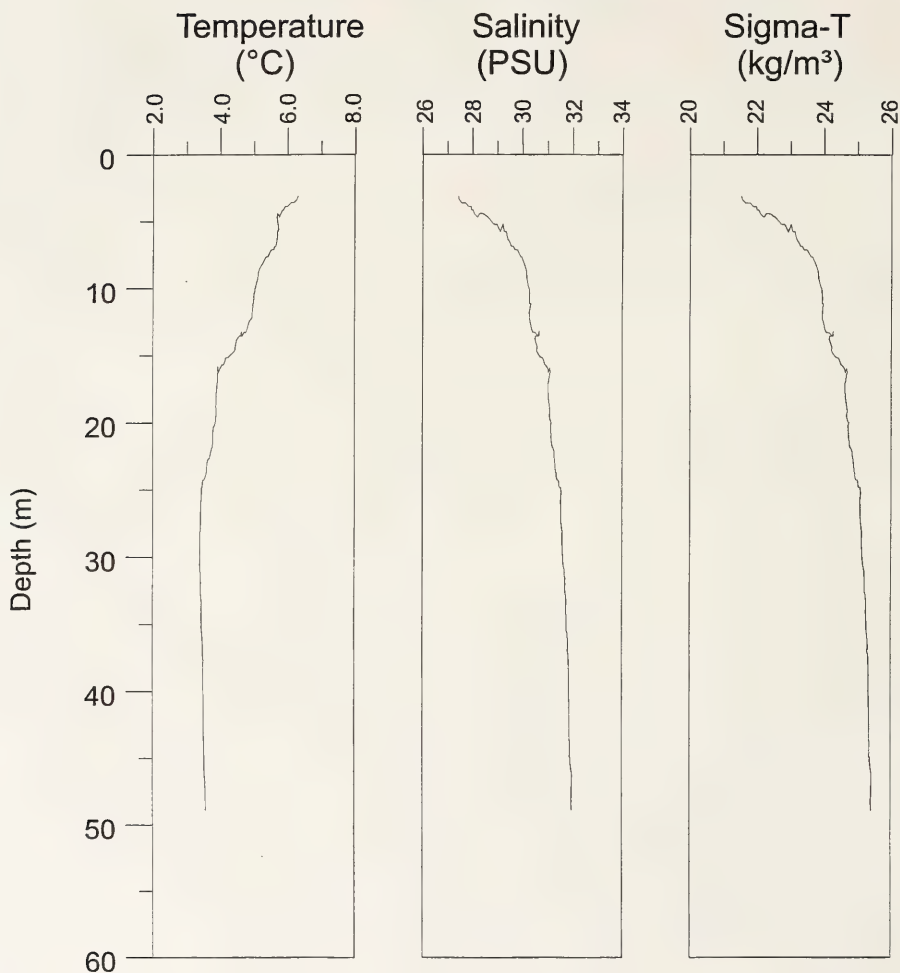


Figure 3-1b. Vertical profiles of temperature, salinity, and density (sigma-t) acquired at the Portland Disposal Site on April 22, 1996. Water depth at the measurement site was 60 m.

discharge. Salinities were less than 28 ppt and temperatures exceeded 6°C within a few meters of the surface. With increasing depth, salinities increased and temperatures decreased, resulting in considerable density stratification over the depth range from 3 to 17 m. Below 25 m, variations in both temperature and salinity were minimal such that the density stratification in the lower half of the water column was very weak, as had been observed in February (Figure 3-1a).

By late spring (May 14), the upper water column had warmed further, resulting in a 20 m-thick layer having temperatures exceeding 6.6°C and salinities in the range from roughly 29 to 31.5 PSU (Figure 3-1c). Beneath a moderate thermocline and pycnocline extending from 20 to 30 m, all water properties were nearly constant throughout the lower 30 m of the water column, as had been observed in February and April.

Comparison of water properties among the three vertical profiles acquired in spring 1996 is best accomplished through analysis of temperature/salinity (T/S) characteristics (Figure 3-2). In this figure, T/S characteristics for each of the three profiles are presented to illustrate the greater range of near-surface water properties during April and May compared with the February profile. It is also interesting to note that bottom waters during February were warmer than the near-surface waters, in contrast to the later profiles which showed coldest waters at the bottom. Near-bottom salinities were always higher than near-surface salinities, although the vertical salinity gradients were much greater in late spring due to river runoff. Overall, near-bottom temperature, salinity, and density had not varied greatly during the spring measurement period, which extended from late February to mid-May 1996; near-surface water properties had, however, changed considerably due to river runoff and vertical mixing to depths of 20 m. These results are generally consistent with the seasonal T/S analyses presented by Colton et al. (1968) for the central Gulf of Maine and by Brown and Beardsley (1978) for the coastal region southeast of Portland.

With regard to the vertical density stratification at PDS, it is apparent that the entire water column to a depth of 60 m is very weakly stratified throughout winter and early spring, whereas the introduction of relatively fresh/warm waters at the surface during mid-spring causes considerable stratification that may tend to decouple horizontal currents and other transport processes within a basic two-layer system. Consequently, downward propagation of storm-generated energy would be most effective during winter and late spring when the water column is nearly void of density stratification. With the onset of spring and summer, the bottom waters are less free to mix vertically with the upper layers, and the resulting stratification acts as a partial barrier to the energy imparted by storms. Further discussion of vertical mixing and storm effects on near-bottom currents and material transport is presented in Section 3.3.

Water Column Profiles Portland Disposal Site May 14, 1996

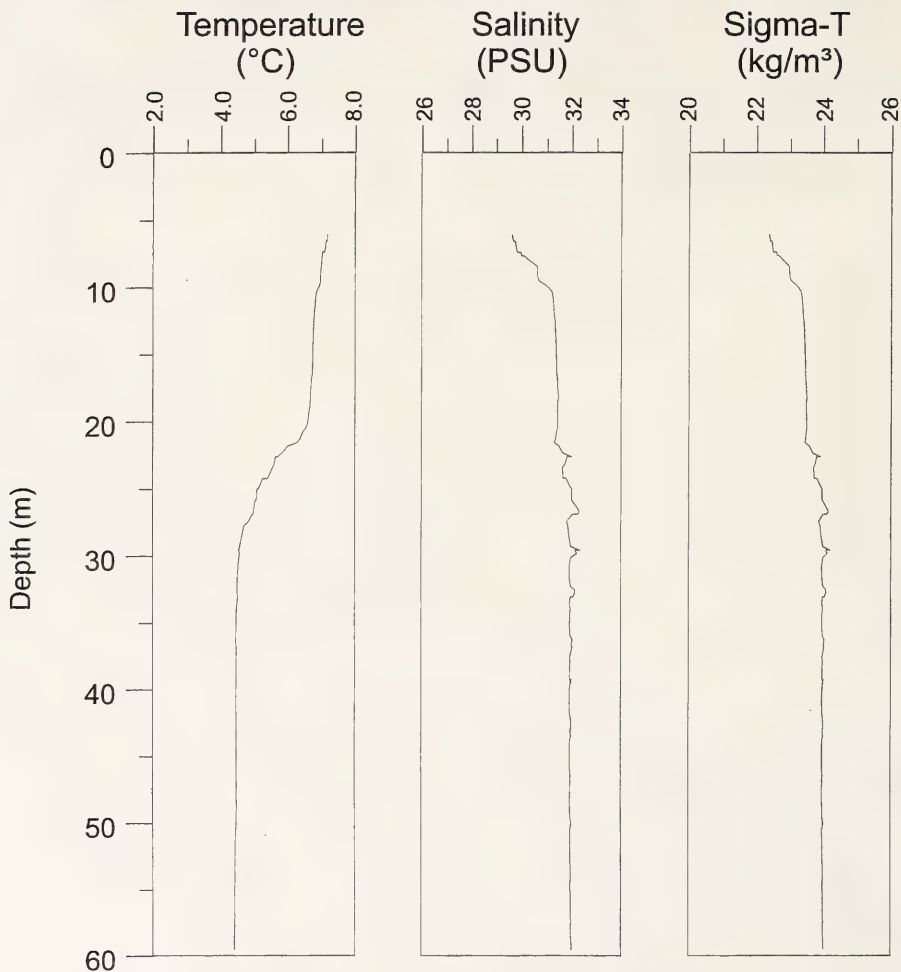


Figure 3-1c. Vertical profiles of temperature, salinity, and density (sigma-t) acquired at the Portland Disposal Site on May 14, 1996. Water depth at the measurement site was 60 m.

Temperature/Salinity Characteristics Portland Disposal Site

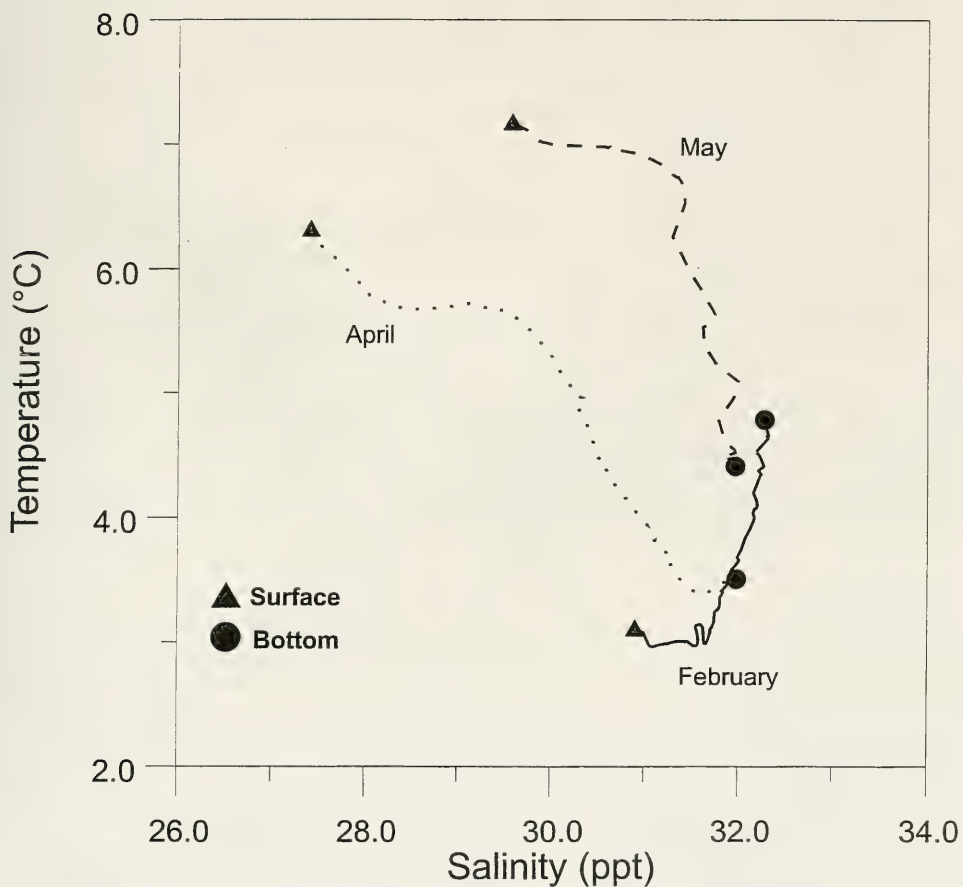


Figure 3-2. Temperature/salinity characteristics of the three vertical profiles (see Figures 3-1a through c) acquired at the Portland Disposal Site during spring of 1996

3.2 Surface Wave Climatology

This section presents meteorological and surface wave data from NOAA buoy 44007 during the period from January 1993 through May 1996. In the discussion which follows, emphasis is placed on wave climatology and the frequency of major storms, as the main objective of this project was to determine whether storm waves can generate significant near-bottom currents and resuspension of bottom sediments at PDS. It is well known that major coastal storms can cause significant perturbations in the internal pressure field of the coastal ocean and intensified, low-frequency currents as a result of this pressure adjustment; discussion of storm-generated currents is presented in Section 3.3.

3.2.1 Time Series of Meteorological Observations

The meteorology along the coast of Maine is seasonally dependent, as reflected by winds, atmospheric pressure fluctuations, surface waves, and water temperature. To illustrate this seasonal variability, Figures 3-3a through 3-3c present annual time series of meteorological and oceanographic conditions measured by NOAA buoy 44007 during 1993, 1994 and 1995, respectively. The most noticeable characteristic of these time series plots is the annual cycle of sea surface temperature (next-to-lowest tier in figures), ranging from a minimum of roughly 1°C in March to a maximum approaching 20°C in July. Short-term temperature fluctuations on the order of a few degrees are observed in summer months, probably as a result of diurnal heating and strong temperature stratification in the near-surface waters. In contrast, surface water temperatures vary minimally on time scales of hours to days during fall and winter on account of intense vertical mixing and creation of a relatively thick isothermal layer at the surface.

Surface waves in the vicinity of PDS (middle two tiers in Figures 3-3a through 3-3c) are largest in fall and winter as a result of storms which normally have durations of a few days. For example, in 1993 ten events having significant wave heights in excess of 4 m were encountered during February-March and during December 1993-January 1994 (Figure 3-3a). Fewer storms having waves in excess of 4 m were observed in 1994 and 1995 (Figures 3-3b and 3-3c, respectively) but all occurred during fall or winter. Wave periods (presented as the period of the most dominant wave in the wave spectra for a given measurement) were generally between 4 and 12 sec, but longer periods were sometimes encountered.

Atmospheric pressure data (lowest tier in Figures 3-3a through 3-3c) reveal larger and more frequent fluctuations during fall and winter, in concert with major fluctuations in wave height and wind speed that were associated with the passage of storms.

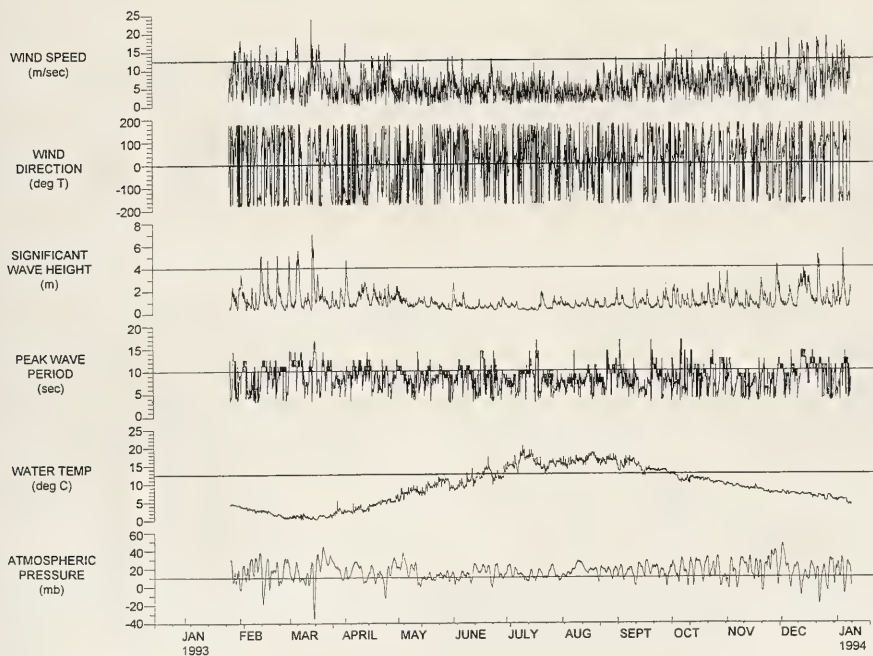


Figure 3-3a. Time series plot of meteorological and wave data from NOAA buoy 44007 during the period from January 1993 to January 1994. The following data (presented as hourly observations) are presented on individual tiers starting from the top: wind speed, wind direction, significant wave height, peak wave period, surface water temperature, and atmospheric pressure (after the mean was removed).

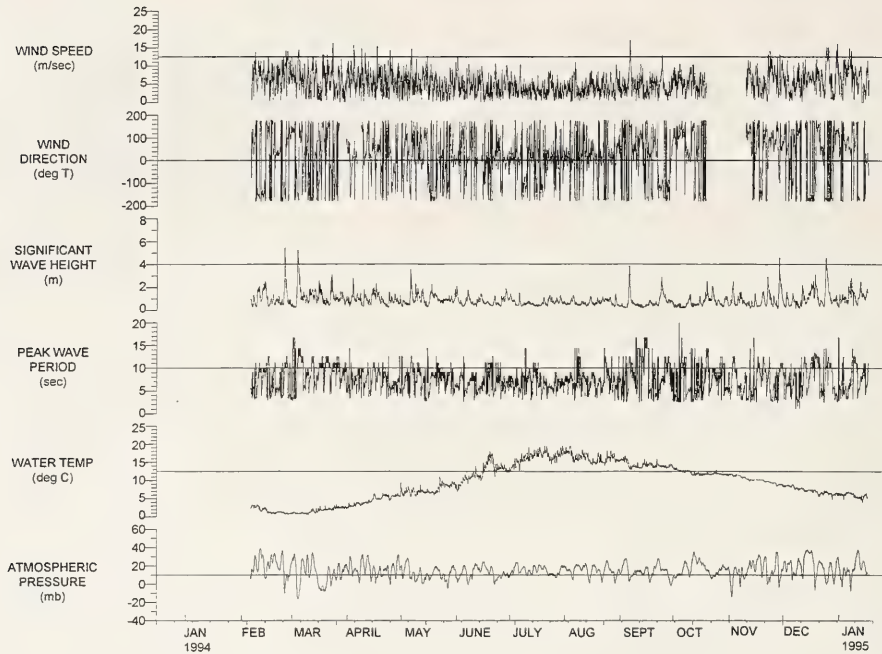


Figure 3-3b. Time series plot of meteorological and wave data from NOAA buoy 44007 during the period from February 1994 to January 1995. The following data (presented as hourly observations) are presented on individual tiers starting from the top: wind speed, wind direction, significant wave height, peak wave period, surface water temperature, and atmospheric pressure (after the mean was removed).

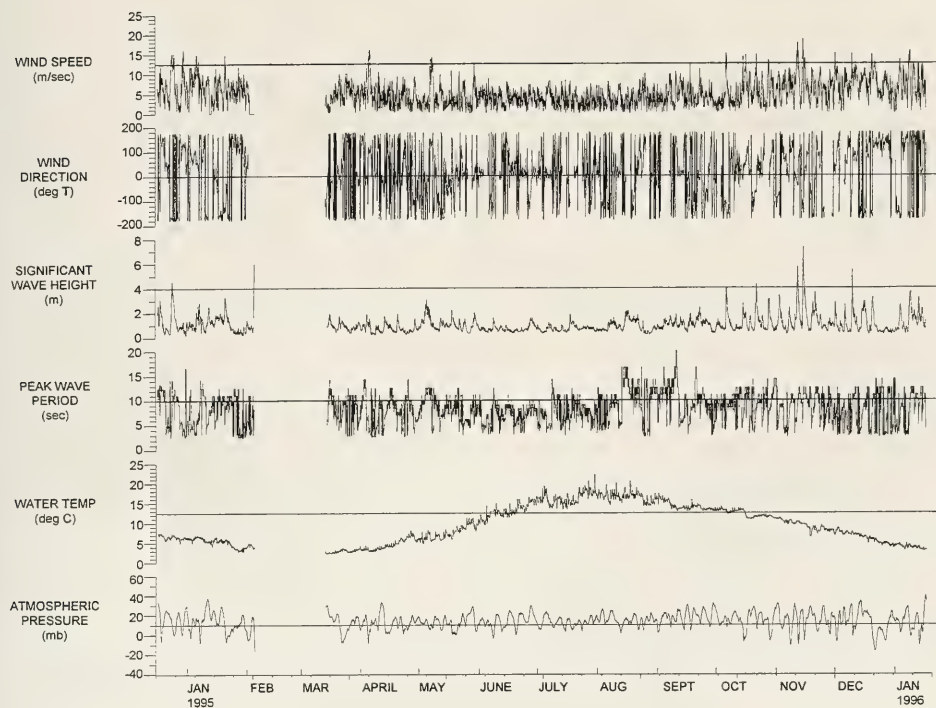


Figure 3-3c. Time series plot of meteorological and wave data from NOAA buoy 44007 during the period from January 1995 to January 1996. The following data (presented as hourly observations) are presented on individual tiers starting from the top: wind speed, wind direction, significant wave height, peak wave period, surface water temperature, and atmospheric pressure (after the mean was removed).

To facilitate comparison of marine meteorological conditions during 1996 with those of prior years, Figure 3-3d presents buoy observations from January through May 1996. Unfortunately, the anemometer on the buoy was inoperable for three time periods during this five-month record, but the wave, water temperature, and atmospheric pressure data are complete, and sufficient for this analysis. During the period from January through May 1996, three events were encountered having significant wave heights in excess of 4 m during winter and late spring (note that this is similar to the amount of storm activity observed during the period from 1993 through 1995).

Also evident in the 5-month buoy time series from 1996 (Figure 3-3d) is a gradual decrease of wave periods from numerous values in excess 10 sec during January through March, to fewer wave periods less than 10 sec thereafter. This seasonal trend toward shorter wave periods in spring and summer can be expected due to less severe storms.

Inspection of the surface water temperature record from 1996 (next to lowest tier in Figure 3-3d) reveals that 10°C water was encountered on May 22, which was one to two weeks earlier than during the prior three years. This may reflect a somewhat milder winter/spring in 1996, but this would not affect the processes governing near-bottom currents and sediment resuspension at PDS.

3.2.2 Annual Wave Statistics

The time series results from the NOAA buoy illustrated that 1993 contained more storm activity than either 1994, 1995, or the first five months of 1996. To facilitate analysis of the interannual variability in wave characteristics in the vicinity of PDS, frequency distribution tables of the percent frequency of occurrence of significant wave height versus peak (most dominant) wave period are presented in Appendix A for each of the four years from 1993 through May of 1996. To summarize the annual wave statistics, Table 3-1 presents the percentage of time (per year) that hourly observations of significant wave heights were within various 1-m wave height ranges. For example, wave heights ranging from 3 to 4 m were observed 1.8% of the time in 1993 versus 1.0% of the time in 1995, with results from the 3 complete record years being very similar. Three- to 4-meter waves were observed more often (2.4%) during 1996, but this was partially a result of summer and fall data not having been included in the 1996 data.

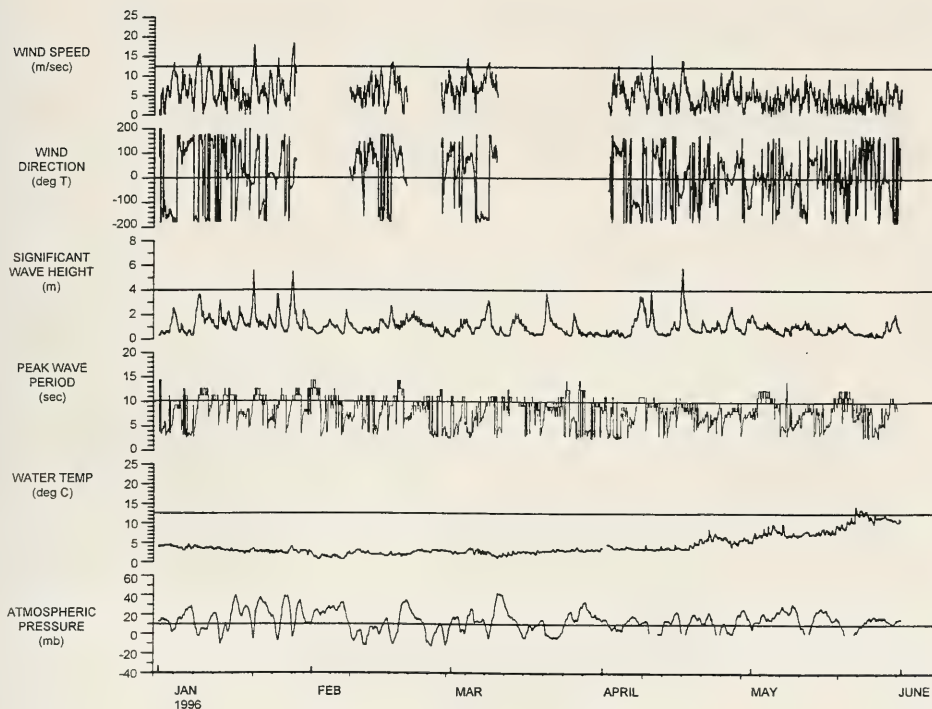


Figure 3-3d. Time series plot of meteorological and wave data from NOAA buoy 44007 during the period from January through May 1996. The following data (presented as hourly observations) are presented on individual tiers starting from the top: wind speed, wind direction, significant wave height, peak wave period, surface water temperature, and atmospheric pressure (after the mean was removed).

Table 3-1

Annual Statistics of Significant Wave Heights for the Period from January 1993 through May 1996 as Observed by NOAA Buoy 44007

Upper: Percent Occurrence of Hourly Observations within Specific Wave Height Ranges.

Middle: Duration (hours) of Significant Wave Heights above Specific Wave Heights.

Lower: Maximum Significant Wave Height.

Percent of Hourly Observations

	1993	1994	1995	1996*
7	0.0	0.0	0.1	0.0
6	0.3	0.2	0.2	0.2
5	1.1	0.4	0.3	0.6
4	1.8	0.8	1.0	2.4
3	6.9	3.8	4.7	6.8
2	30.3	26.2	32.5	37.3
1	59.5	68.6	61.4	52.7
0				

Duration (total hours per year)

	1993	1994	1995	1996*
> 3 m	261	113	126	117
> 4 m	114	49	47	29
> 5 m	24	16	24	7
> 6 m	0	0	8	0

Maximum
Significant
Wave
Height (m)

1993	1994	1995	1996*
7.0	5.6	7.3	5.8

* Data from January through May only.

Overall, the year-to-year wave results are very similar, showing that significant wave heights are less than 2 m from 90 to 95% of the time during each year. Larger waves were more prevalent during 1993 as discussed above. As shown in the middle portion of Table 3-1, the duration (expressed as total hours per year) of large waves in 1993 was roughly twice that of the following few years for wave heights between 3 and 5 m; for larger waves, interannual differences were less pronounced. The maximum significant wave height observed in each of the four measurement years ranged from 5.6 to 7.3 m (lower portion of Table 3-1).

From this analysis it appears that wave characteristics during the first half of 1996 were typical of other recent years at this location.

3.2.3 Seasonal Wave Statistics

To further investigate the seasonal variability of wave conditions in the vicinity of PDS, the frequency distribution of hourly significant wave height versus wave period has been computed for four seasons using the 3.4 years of buoy data. Seasons have been defined as winter (December-February); spring (March-May); summer (June-August); and fall (September-November). Whereas the frequency distribution statistics for each season are provided in Appendix B, a summary of the key results is presented in Table 3-2 and listed below:

- Mean significant wave heights in winter (1.22 m) are nearly twice those in summer (0.68 m), while mean wave heights in spring and fall are approximately 1 m.
- Maximum significant wave heights in summer were 2.7 m, compared to 6.0 m in winter and approximately 7 m in spring and fall.
- Mean wave periods were approximately 8 sec during all seasons, but the standard deviation was approximately 3 sec.
- Significant wave heights exceeded:
 - 1 m only 16.6% of the hourly observations in summer, compared to 38 to 52% in winter, spring, and fall.
 - 3 m 4.4% of the hourly observations in winter, compared to roughly 2% in spring and fall, and 0% in summer.
 - 5 m 0.2-0.3% of the hourly observations in winter, spring, and fall, compared to 0% in summer.

Table 3-2

Seasonal Wave Statistics for the Period from January 1993 through May 1996
as Observed by NOAA Buoy 44007

	Mean Wave Height (m)	Maximum Wave Height (m)	Mean Wave Period (sec)	Percent of Wave Height Observations		
				> 1 m	> 3 m	> 5 m
Winter	1.22	6.00	8.16	52.1	4.4	0.3
Spring	1.06	7.00	8.27	45.0	2.5	0.3
Summer	0.68	2.70	7.69	16.6	0.0	0.0
Fall	0.97	7.30	8.25	38.5	2.0	0.2

3.2.4 Duration of Storm Waves

As illustrated in the time series of significant wave heights for the 3.4 years of data from NOAA buoy 44007 (Figures 3-3a through 3-3d), the duration of large waves during the passage of major storms is relatively brief, often persisting for only a fraction of a day. A quantitative analysis of the duration of waves within specific height ranges (Table 3-3) reveals that waves greater than 3 m had average durations of 6 to 8 hrs; waves in this height range were observed on 72 (31 + 15 + 26) occasions for a total of 562 hours (approximately 165 hrs or 7 days per year). In contrast, wave heights greater than 5 m were observed only 22 times, with average durations of only 1 to 3 hrs, for a total of 59 hrs. Therefore, although large waves are not uncommon in the vicinity of PDS, they normally do not persist for long periods of time.

3.2.5 Meteorological Conditions during Spring of 1996

Meteorological and wave conditions during spring of 1996 were similar to spring conditions during the three prior years (see Section 3.2.3). As indicated in the time series of observations from NOAA buoy 44007 during the period from March through May 1996 (Figure 3-4), there was a gap in the wind record from March 10 to April 1, but the available wind data illustrate typical, synoptic fluctuations in wind speed on time scales of hours to a few days, the latter being associated with the passage of large-scale meteorological systems. Wind speeds approached 34 mph (15 m/sec) on a few occasions, but these maximum winds persisted for only a few hours during the individual storms. Three-hour low pass filtered wind vectors during spring of 1996 (second tier from the top in Figure 3-4) illustrate the high

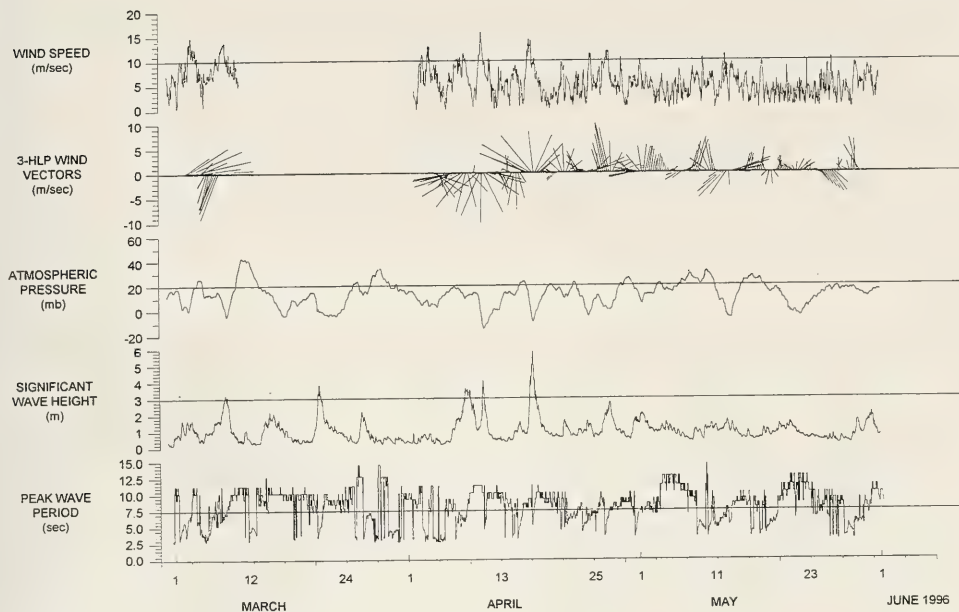


Figure 3-4. Time series plot of meteorological and wave data from NOAA buoy 44007 during the period from March through May 1996, corresponding with the period of the oceanographic measurement program. The following data (presented as hourly observations) are presented on individual tiers starting from the top: wind speed, wind vectors, atmospheric pressure (after the mean was removed), significant wave height, and peak wave period.

degree of wind direction variability, typically on time scales of the synoptic meteorology (i.e., 2-4 days). Close inspection of the wind vector record reveals that on April 17, the large storm waves were associated with low atmospheric pressure and strong southerly winds. In contrast, the storms on April 8 and 10 caused strong northeasterly and northerly winds, respectively.

The wave records from March through May 1996 (lower two tiers in Figure 3-4) illustrate five storm events attaining significant wave heights greater than 3 m, one of which (on April 17) had waves exceeding 5 m.

Table 3-3

Duration Intervals and Significant Wave Heights of Major Storms during the Period from January 1993 through May 1996 as Observed by NOAA Buoy 44007

Time Period		Significant Wave Height (m)				
		>3	>4	>5	>6	>7
1/93 - 1/94	Events	31	18	11	1	0
	Ave. Duration (hr)	8	6	2	3	
	Total (hr)	263	122	28	3	
2/94 - 2/95	Events	15	6	4	0	0
	Ave. Duration (hr)	6	5	1		
	Total (hr)	96	32	7		
3/95 - 5/96	Events	26	14	7	3	1
	Ave. Duration (hr)	7	4	3	1	1
	Total (hr)	203	67	24	4	1

3.3 Assessment of Currents and Physical Processes

3.3.1 Analysis of Near-Bottom Currents

The three consecutive deployments of moored instrumentation at PDS yielded nearly complete records of near-bottom currents, water temperature, pressure, and relative turbidity over the period from February 27 to May 14, 1996. To illustrate the temporal variability in

these independent parameters, Figure 3-5 presents time series results from the entire measurement program. Inspection of the pressure record (third tier from the bottom in Figure 3-5) reveals data gaps on April 6 and 22 associated with servicing of the instrumentation. Also evident is the shift in mean pressure associated with each redeployment of the instrumentation, which is a result of deployment at a slightly different location and water depth (see discussion of local bathymetry in Section 2.1.2). Aside from the pressure (depth) offsets between these three pressure records, we see the periodic semi-diurnal fluctuations in water level having a range of 3.5 m during the spring tide period.

The water temperature record from February to May (fourth tier from the bottom in Figure 3-5) exhibits considerable variability over the range from 3.6° to 5.5°C. Semi-diurnal temperature fluctuations on the order of a few tenths of degrees were evident during the first three weeks of March, presumably due to tides (either vertical excursions within a near-bottom thermocline, or horizontal displacement of water parcels within a region of horizontal temperature gradients). Later in the deployment period, short-term fluctuations were practically nonexistent, especially during the period from April 18 to May 4 which was characterized by isothermal water of 4.1°C. The consistency of this temperature reading was initially considered suspect, but as it spanned two deployment periods (at slightly different locations) it is highly probable that the mooring region contained a considerable near-bottom layer of isothermal water which was advected away after May 5. This thick layer of 4°C water was evident from the CTD profile acquired on April 22 (see Section 3.1). Overall, the near-bottom water temperatures measured by the CTD profiler on February 27, April 22, and May 14 were consistent with the moored temperature record, although the CTD values were consistently 0.4°C lower than the thermistor on the S4 current meter.

Hourly averaged near-bottom current speed during the February to May measurement period (upper tier in Figure 3-5) ranged from approximately 0 to 20 cm·s⁻¹, with the majority of the variability occurring at periods of approximately 12 hr in association with the semi-diurnal tide. Significant aperiodic variability in current speed was observed on time scales ranging from hours to a few days, possibly related to atmospheric forcing. Mean current speeds for each of the three deployments were similar (near 7 cm·s⁻¹), but the third deployment period (from April 23 to May 14) was characterized by significantly less speed variability than the first two deployment periods, while the second deployment period (from April 6 to 22) exhibited the largest speed variability. The noticeable changes in current speed characteristics at both of the instrument servicing events (April 6 and 22) suggest that redeployment of the instrumentation had an effect on the subsequent current measurements. This is even more obvious upon inspection of the current direction data (second tier from the top in Figure 3-5), which shows relatively consistent flow toward -60° (300°T) during the third deployment, dominant flow toward 140°T during the first deployment, and flow toward -150° (210° T) during the second deployment.

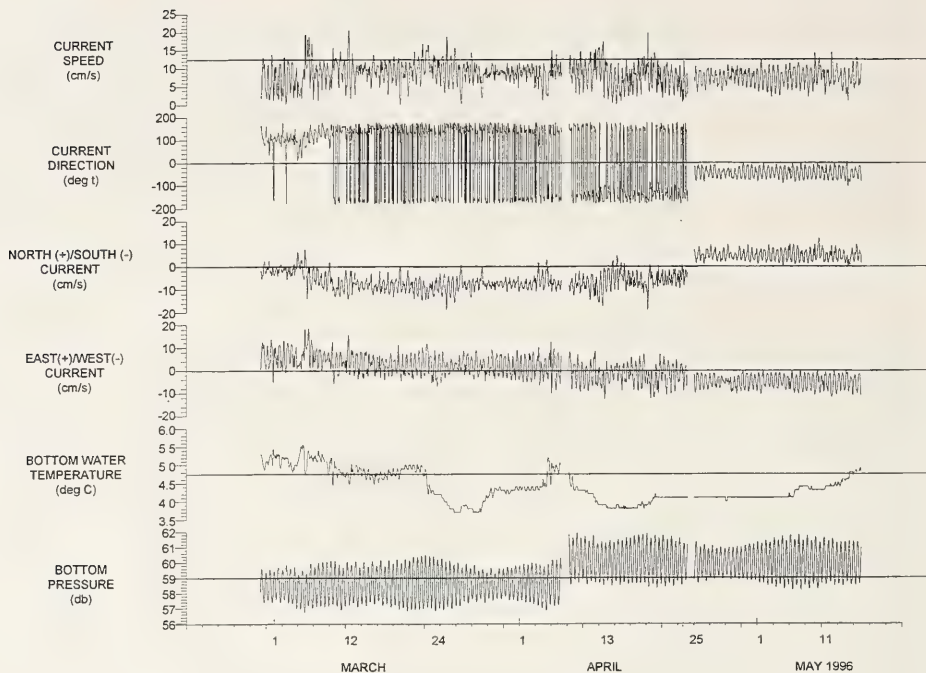


Figure 3-5. Time series plot of near-bottom data acquired during the 3-month measurement period. The following data are presented on individual tiers starting from the top: hourly current speed, hourly current direction, north(+)/south(-) component of the near-bottom current, east(+)/west(-) component of the near-bottom current, near-bottom water temperature, and near-bottom pressure.

Decomposition of the current data into north-south (V) and east-west (U) components (third and fourth tiers from the top of Figure 3-5, respectively) further illustrates the directional shift among the three deployment periods. Currents had a southward (-V) component during most of the first and second deployments, whereas current vectors consistently had a northward (+V) component during the third deployment. The east-west current component demonstrated a gradual shift from mostly eastward (+U) currents to purely westward (-U) currents over the 3-month measurement period. The decrease in the amplitude of the temporal variability in currents from February to May is evident in both current vector components.

To further investigate this shift in near-bottom flow direction that corresponded with servicing of the instrumentation, Figure 3-6 presents time series of near-bottom pressure, water temperature, and current vectors for the entire deployment period. The shift from southeastward flow to southwestward flow, then to northwestward flow is striking. Notice, however, that at the beginning of the measurement program, near-bottom currents shifted abruptly from eastward to southward within a period of a few days, demonstrating that it is possible for low-frequency (longer than tidal period) currents at this location to change directions on time scales of a day or less.

Another interesting point that is evident from Figure 3-6 is that water temperatures generally decreased during the first three weeks of the program while the flow was offshore (southward).

The CTD profile data from February 27, 1996 (see Figure 3-1a) illustrated that water temperatures in the near-surface layers were colder than those near the bottom. Consequently, if the near-bottom flow was directed offshore (generally downslope toward the south), it is possible that the relatively cold waters residing at shallow depth inshore of the mooring site could have moved downslope, causing the gradual reduction in water temperatures at the mooring site.

During the latter half of the third deployment period, near-bottom water temperatures began to rise during a three-week period of persistent northwestward (onshore) flow. Comparison of the near-bottom water temperatures determined from the CTD profiles on April 22 and May 14 (see Figure 3-2) indicates that temperatures were 1.3°C warmer in May and that a 30-m thick layer of roughly 4.5°C water had displaced the relatively colder water that resided at the mooring site in late April. In the absence of CTD profile data over a broad area at different times during the mooring instrument program, we cannot be sure of the origin of each water type, but it appears possible that the near-bottom warming in early May was, in fact associated with northward (onshore) advection of relatively warmer water from the central Gulf of Maine.

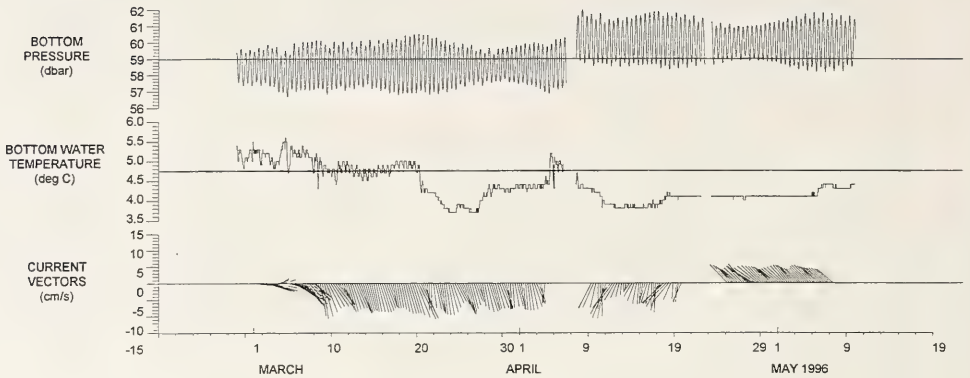


Figure 3-6. Time series plot of bottom pressure (upper tier), near-bottom water temperature (middle tier), and near-bottom current vectors (lower tier) during the 3-month measurement period

From the above analysis of near-bottom water temperature and flow direction, it seems plausible that the striking differences in mean flow direction among the three deployment periods are real. There are, however, three possible scenarios that could have contributed to this abrupt change in current characteristics between deployments:

1. The near-bottom currents actually changed abruptly during the two brief servicing events.
2. The tripod containing the current meter was placed at different locations for each deployment, and because of the extremely rough topography (rock ledges and isolated rocks) the tripod may, for each deployment, have resided very close to different small-scale topographic features rising a few meters above the bottom. If so, it is likely that the currents 46 cm above the seafloor were greatly affected by the local topography and obstructions to flow.
3. The S4 electromagnetic current meter was, for some reason unknown to SAIC or the manufacturer, adversely affected by the magnetic characteristics of the seafloor at the measurement site.

While the current records suggest that mean near-bottom current directions differed significantly during each of the three deployments, we wish to investigate whether the fluctuating component of the currents (due to tides and high-frequency processes) also differs among the three records. As a first step, the mean current vector for each of the three deployment periods was determined:

	Mean Speed ($\text{cm}\cdot\text{s}^{-1}$)	Mean Direction ($^{\circ}\text{T}$)
Deployment 1:	7.4	154
Deployment 2:	6.6	196
Deployment 3:	7.0	312

Although the mean current directions were different among the three deployments, the mean speed was very consistent ($7.0 \pm 0.4 \text{ cm}\cdot\text{s}^{-1}$) among the deployments. As seen in the lower tier of Figure 3-6, the fluctuations in currents superimposed on the mean flow during each of the three deployments are relatively small compared to the means. To determine whether tidal processes are responsible for the majority of these temporal fluctuations, tidal harmonic analyses were conducted on the current records from both the first and third deployment periods, which had 37- and 20-day durations, respectively. For these analyses, the amplitude and phase of the tidal current for each of the tidal harmonic constituents was determined from the time series record; then the results from this constituent analysis were used to predict the magnitude and direction of the oscillatory tidal vectors for the time period of the measurements. Note that in a single current record there can be a wide variety of

physical processes that contribute to the observed variability in speed and direction and, consequently, it is sometimes difficult to resolve the exact contribution of a tidal constituent versus energy from other processes having equal or similar periods. This is especially true if the tidal amplitude is small as is the case for the Portland measurement site.

The tidal analysis of the two deployment periods revealed that near-bottom tidal currents at this location are very weak and predominantly driven by the M_2 semi-diurnal constituent. The amplitude of the near-bottom M_2 tidal current constituent for both the first and third deployments in spring of 1996 was approximately $3 \text{ cm}\cdot\text{s}^{-1}$ compared to amplitudes less than $0.5 \text{ cm}\cdot\text{s}^{-1}$ for all other semi-diurnal and diurnal constituents. This is consistent with past reports of weak ($3\text{-}7 \text{ cm}\cdot\text{s}^{-1}$) tidal currents 1.5 m above the bottom at PDS (NUSC 1979) and at mid-depth in the water column at a site northeast of PDS (Vermersch, Beardsley, and Brown 1979).

The results of the tidal harmonic analysis also can be used to construct tidal current ellipses which represent the speed and direction of the tidal current vector during one period of a specific tidal constituent. Figure 3-7 presents a composite of tidal current ellipses for the M_2 constituent derived from the first and third deployment periods. Note that the ellipse describes the path taken by the end of the tidal vector with its origin at the center of the axes; the speed of the tidal current (in $\text{cm}\cdot\text{s}^{-1}$) is proportional to the scale presented on the axes. As illustrated in this figure, the M_2 tidal current vectors rotate around the predicted ellipse in a counterclockwise direction at a period of 12.42 hr. The major axis of the M_2 tidal current for the first deployment is oriented east-west, whereas, the axis is shifted by 23° for the third deployment. Considering the small amplitude of the tidal currents and the much shorter duration (and presumably less statistical confidence in the tidal analysis) of the third deployment, the results of the tidal analyses of the two deployment periods are reasonably consistent. Ellipses of the other tidal constituents are not shown as their amplitudes are too small to be significant and coherent.

The observed consistency in tidal currents between the first and third deployments contributes significantly to our confidence in the quality of the moored current records. Although the mean flow directions differ greatly among the deployments, the mean speed and the tidal current characteristics for each deployment are consistent. For the remainder of this report, the analyses focus on the near-bottom current variability due to processes other than the tides.

As a first step in the investigation of non-tidal processes, one can vectorally subtract the tidal current components from the observed current records to assess the "residual" currents due to other processes. For example, Figure 3-8 presents an analysis of the residual current amplitude in the north-south (V) and east-west (U) current vector components. The

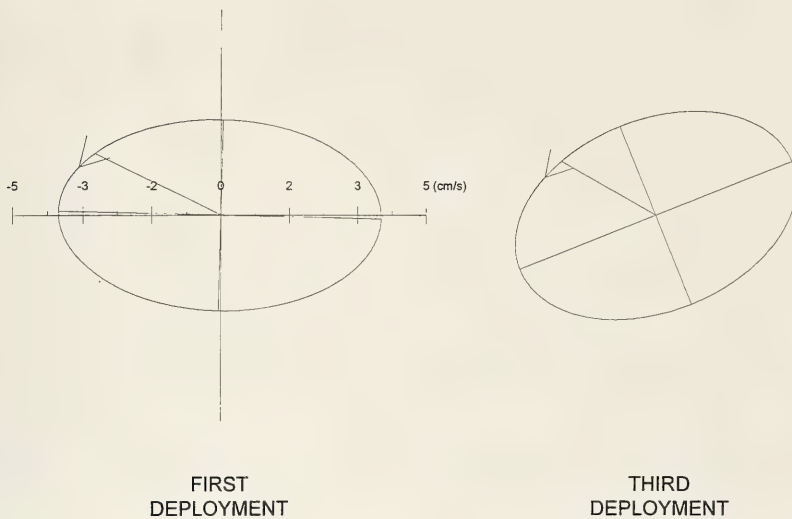
M_2 Tidal Current Ellipses

Figure 3-7. Tidal current ellipses for the M_2 semidiurnal tidal constituent for the first (left) and third (right) deployment periods. The x and y axes are proportional; current speeds are indicated in cm/s. Both ellipses demonstrate that M_2 tidal currents rotate in a counterclockwise direction at the measurement site.

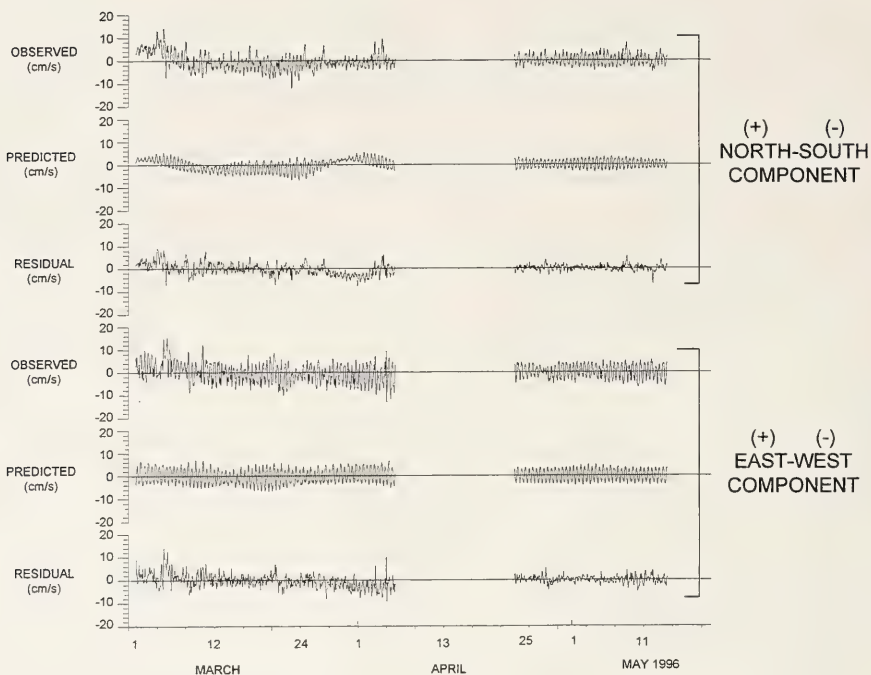


Figure 3-8. Time series plot of hourly observed currents (after the mean had been removed), predicted tidal currents, and residual (observed minus predicted) currents for the first and third deployment periods

observed currents (first and fourth tiers from the top in Figure 3-8) are presented after removal of the mean for each deployment. The predicted tidal currents (second and fifth tiers from the top) illustrate the amplitude of the predicted tidal current in each vector component. The residual (observed minus predicted) currents therefore represent all remaining current fluctuations, regardless of frequency. These residual currents are clearly weak (generally less than $5 \text{ cm}\cdot\text{s}^{-1}$ for each vector component) and composed primarily of high-frequency fluctuations having periods of hours. There is a conspicuous absence of significant events having periods of 2 to 4 days, which normally dominate coastal current records in response to atmospheric forcing during the passage of storms.

Upon first assessment of these residual current records, we were surprised that the storms which generated surface waves as high as 3 to 5 m had almost no effect on the hourly averaged, near-bottom currents at PDS. This result is, however, consistent with results from past current measurements in the western Gulf of Maine which showed that currents in the upper 100 m of the water column are not coherent with local winds and storm events (Vermersch, Beardsley, and Brown 1979). It is believed that currents associated with relatively energetic, baroclinic features are not coherent with local winds. The unusually rough bottom topography in the western Gulf of Maine may interact with the coastal flow to produce baroclinic eddies having a wide variety of vertical and horizontal length scales due to the irregular characteristics of the seafloor topography. If so, these eddies would contribute considerable high-frequency energy to the moored current records at PDS.

The absence of low-frequency energy and the frequent occurrence of high-frequency fluctuations in the near-bottom currents records from PDS support the hypotheses outlined above regarding the processes governing the currents in the vicinity of PDS.

As a final illustration of the lack of coherence between storms and near-bottom currents at PDS, Figure 3-9 presents hourly current speed and direction data (both including the mean and after the mean had been removed), and surface wave characteristics as measured by NOAA buoy 44007. The significant wave height record is a good indicator of the date, duration, and intensity of the numerous storm events that affected the region during March to May 1996. Comparison of the current vectors and the significant wave heights (fifth and sixth tiers from the top in Figure 3-9, respectively) illustrates that hourly averaged near-bottom currents were not intensified during the storm events.

3.3.2 Analysis of Near-Bottom Turbidity

As described in Section 2.2, the relative turbidity of the near-bottom water at PDS was monitored by two optical turbidity sensors mounted in close proximity to the current meter on the tripod. The turbidity sensors were situated at heights of 33 and 81 cm above

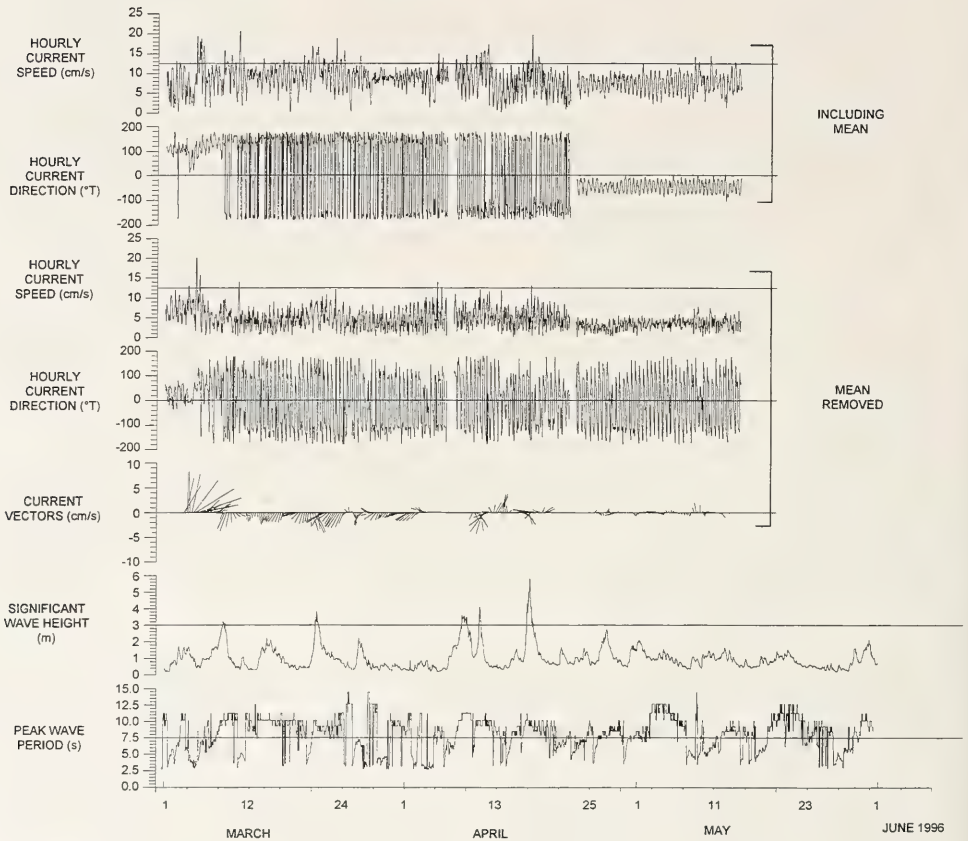


Figure 3-9. Time series plot of near-bottom current data and surface wave data during the 3-month measurement period. The following data are presented on individual tiers starting from the top: hourly current speed, hourly current direction, hourly speed after the mean current vector has been removed from each of the three deployment records, hourly current direction after the mean current vector has been removed, current vectors after the mean has been removed, significant wave height, and peak wave period.

the seafloor to acquire data from two levels and provide basic redundancy in the event that one sensor malfunctioned or became fouled or obstructed.

Time series results from both turbidity sensors are presented in Figure 3-10, in addition to records of significant wave height, near-bottom water temperature, and near-bottom current speed (after the mean had been removed for each deployment period). Both turbidity records illustrate low background turbidity levels throughout the three deployments, with the majority of the measurements lying below $5 \text{ mg}\cdot\text{l}^{-1}$. The maximum observed turbidity during the measurement period was roughly $160 \text{ mg}\cdot\text{l}^{-1}$, as measured by the lower sensor on April 5. It is, however, likely that this measurement was erroneous due to a temporary physical obstruction to the optical sensor pathway (e.g., seaweed caught on the sensor or supporting bracket) rather than gradual biofouling of the sensor, as the high values were achieved suddenly and with no concurrent elevation in turbidity at the other sensor situated only 48 cm above.

Two other major events, characterized by elevated turbidity levels at both sensor levels, are apparent on April 9 and 17 (Figure 3-10). As discussed in further detail below, these data truly represented elevated turbidity levels in the lower water column that resulted from oscillatory currents generated by storm waves. Additional events having slight elevations in near-bottom turbidity occurred during the measurement program, but are not evident in Figure 3-10 due to the coarse scale of the turbidity axis.

3.3.3 Analysis of Near-Bottom Currents and Turbidity during Storm Events

Previous sections demonstrated that significant storms did pass over PDS during the period from February 27 to May 14, 1996, but the hourly averaged currents exhibited no intensification due to the storms. The simultaneous occurrence of large surface waves and elevated near-bottom currents during at least a few major storms raises the question of what physical mechanism is responsible for the high turbidity levels. Could the energy of the storm-generated waves penetrate to the seafloor within PDS causing significant, oscillatory near-bottom currents that resuspended ambient sediment? Or could the elevated near-bottom turbidity be a result of horizontal transport of material that had been resuspended elsewhere? To investigate these hypothetical processes and their frequency of occurrence at the measurement site, we have identified nine separate storm events during the February to May 1996 deployment period which had maximum significant wave heights of at least 2 m (Table 3-4). Time series plots presenting surface wave and near-bottom current, water temperature, and turbidity data during each storm event are presented in Figures 3-11a through 3-11i to illustrate short-term fluctuations in each parameter as well as their potential coherence.

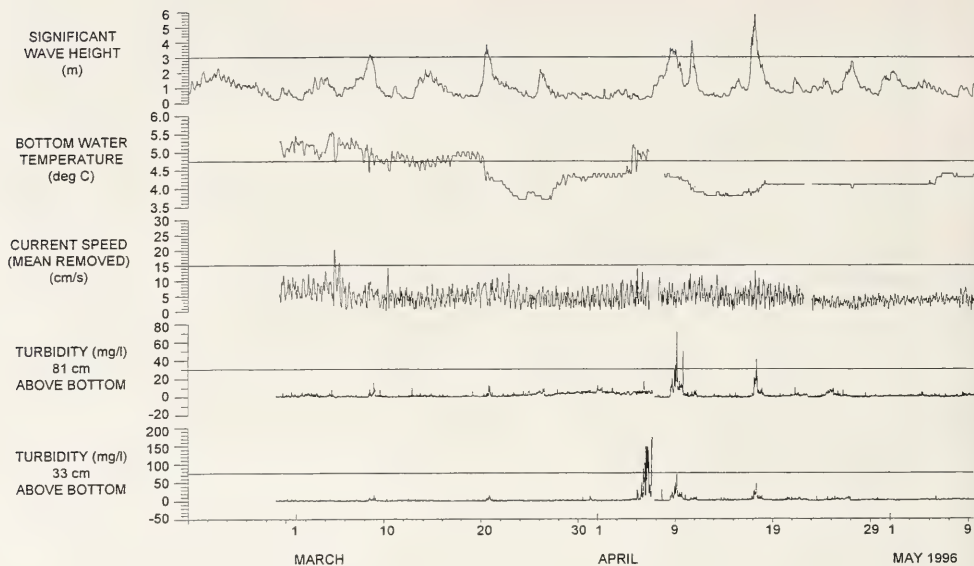


Figure 3-10. Time series plot of data from the 3-month measurement period. The following data are presented on individual tiers: significant wave height, near-bottom water temperature, hourly current speed after the mean has been removed from each of the three deployment records, and turbidity at 81 cm (upper) and 33 cm (lower) above the seafloor.

Table 3-4

Summary of Maximum Wave Heights, Peak Wave Periods, Duration of Wave Heights Greater than 3 m, and Maximum of the Burst-Averaged Standard Deviation in Near-Bottom Current Speeds during Nine Storm Events during the Period from February 27 to May 14, 1996

Storm Event	Date	Significant Wave Height (m)	Peak Wave Period (s)	Duration Wave Ht. > 3 m (hrs)	Max SDCS (cm·s ⁻¹)
1	March 8	3.0	10.8	-	10
2	March 14	3.2	10.8	-	7
3	March 20	3.6	10.0	10	10
4	March 26	2.2	7.0	-	2
5	April 8	3.5	11.1	17	15
6	April 10	4.0	10.0	8	12
7	April 16	5.8	10.0	17	16
8	April 26	2.7	8.1	-	4
9	May 1	2.0	8.3	-	2

As indicated in Table 3-4, four storms (3, 5, 6, and 7) had maximum significant wave heights of 3.5 m or greater, and durations of 8 to 17 hrs when significant wave heights were 3 m or greater and peak wave periods were at least 10 s; the other five storms were less intense. Assessment of the time series results from Storm 3 (Figure 3-11c) reveals that near-bottom turbidities at both sensor levels rose significantly beginning at mid-day on March 20, at approximately the same time as significant wave heights achieved 3 m. As the wave heights fell below 2.5 m about 16 hrs later, near-bottom turbidity values dropped sharply. During this storm event, maximum turbidities (on the order of 10 mg·l⁻¹) at both sensor levels were encountered at approximately the same time, but as expected for near-bottom suspended sediments, the highest turbidity and the longest duration of elevated turbidity levels were encountered closest to the seafloor.

The monotonic progression from short- to long-period (e.g., 5- to 10-sec) waves during storm 3 (Figure 3-11c) suggests that surface wave energy would penetrate to greatest depth near the end of the storm when significant wave heights were still about 3 m while wave periods reached 10 sec. This dependency of sediment resuspension on wave period and height is evident during storm 3 as maximum turbidities occurred after the maximum wave heights were encountered and elevated turbidities persisted for some time thereafter. As

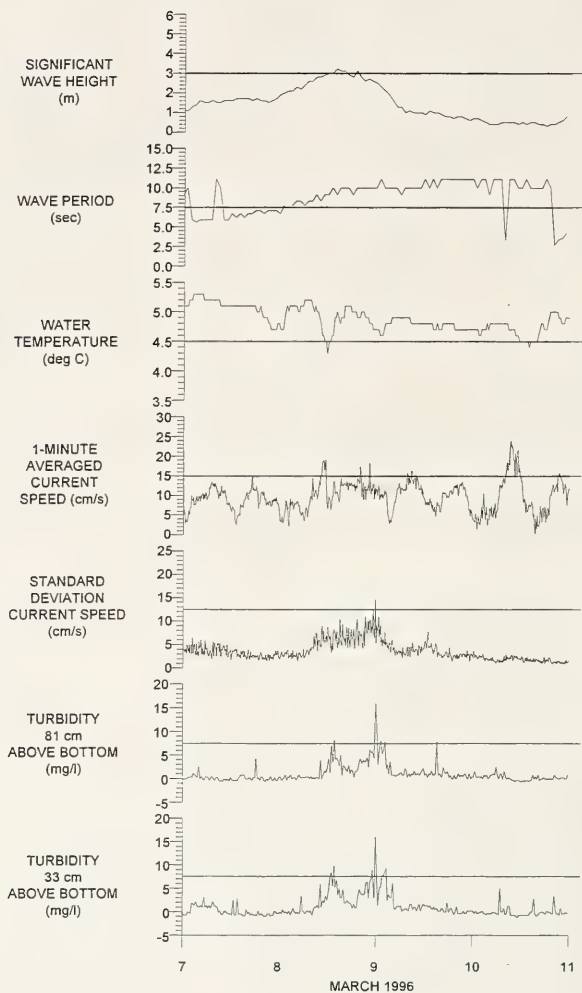


Figure 3-11a. Time series plot of surface wave and near-bottom current and turbidity data during storm 1. The following data are presented on individual tiers starting from the top: significant wave height and peak wave period, near-bottom water temperature, 1-min averaged current speed, the standard deviation in current speed over 1-min periods at 10-min intervals, and turbidity at 81 cm (upper) and 33 cm (lower) above the seafloor.

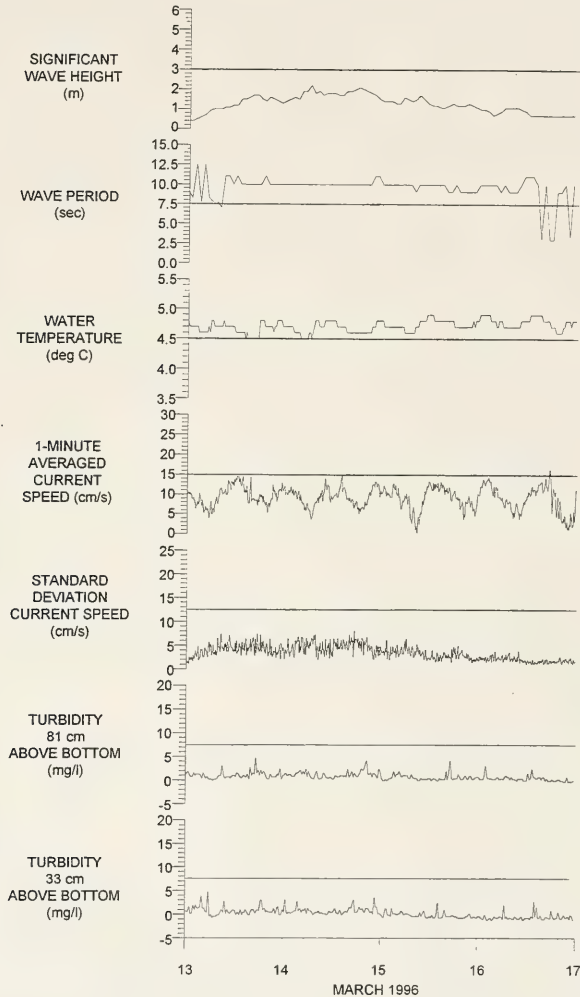


Figure 3-11b. Time series plot of surface wave and near-bottom current and turbidity data during storm 2. The following data are presented on individual tiers starting from the top: significant wave height and peak wave period, near-bottom water temperature, 1-min averaged current speed, the standard deviation in current speed over 1-min periods at 10-min intervals, and turbidity at 81 cm (upper) and 33 cm (lower) above the seafloor.

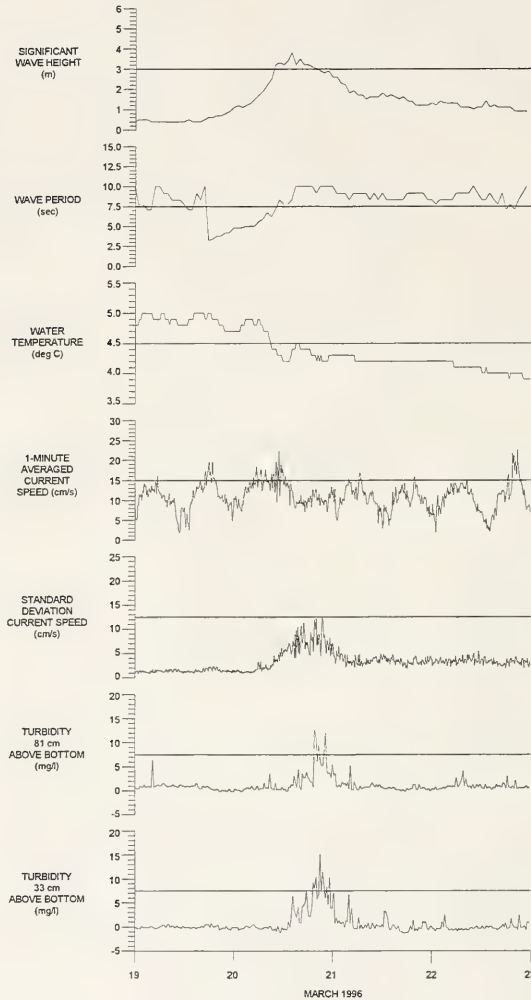


Figure 3-11c. Time series plot of surface wave and near-bottom current and turbidity data during storm 3. The following data are presented on individual tiers starting from the top: significant wave height and peak wave period, near-bottom water temperature, 1-min averaged current speed, the standard deviation in current speed over 1-min periods at 10-min intervals, and turbidity at 81 cm (upper) and 33 cm (lower) above the seafloor.

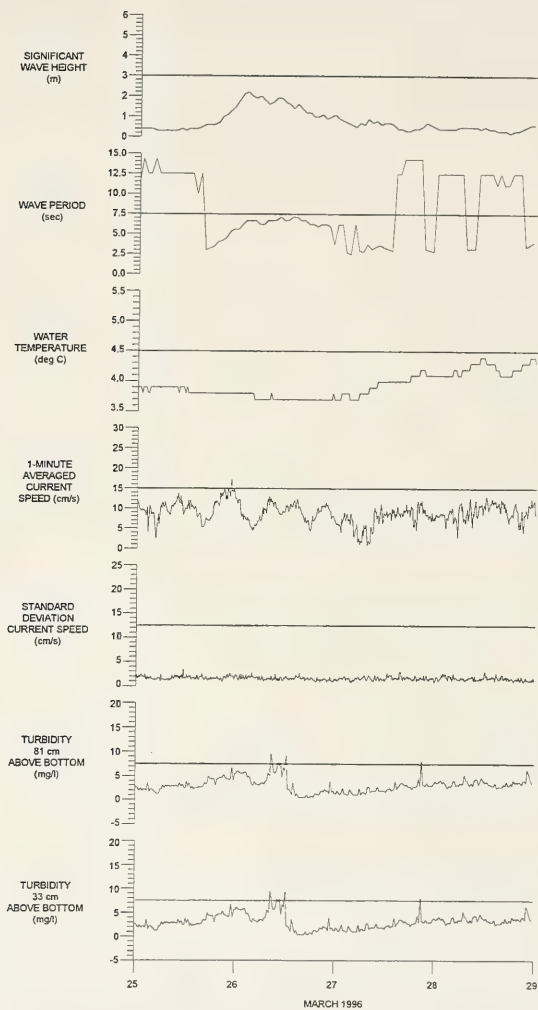


Figure 3-11d. Time series plot of surface wave and near-bottom current and turbidity data during storm 4. The following data are presented on individual tiers starting from the top: significant wave height and peak wave period, near-bottom water temperature, 1-min averaged current speed, the standard deviation in current speed over 1-min periods at 10-min intervals, and turbidity at 81 cm (upper) and 33 cm (lower) above the seafloor.

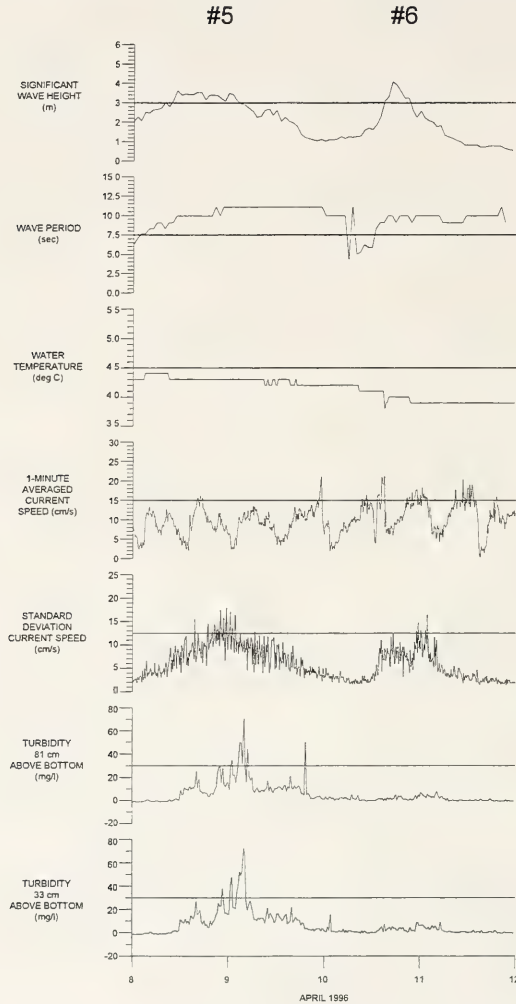


Figure 3-11e. Time series plot of surface wave and near-bottom current and turbidity data during storms 5 and 6. The following data are presented on individual tiers starting from the top: significant wave height and peak wave period, near-bottom water temperature, 1-min averaged current speed, the standard deviation in current speed over 1-min periods at 10-min intervals, and turbidity at 81 cm (upper) and 33 cm (lower) above the seafloor.

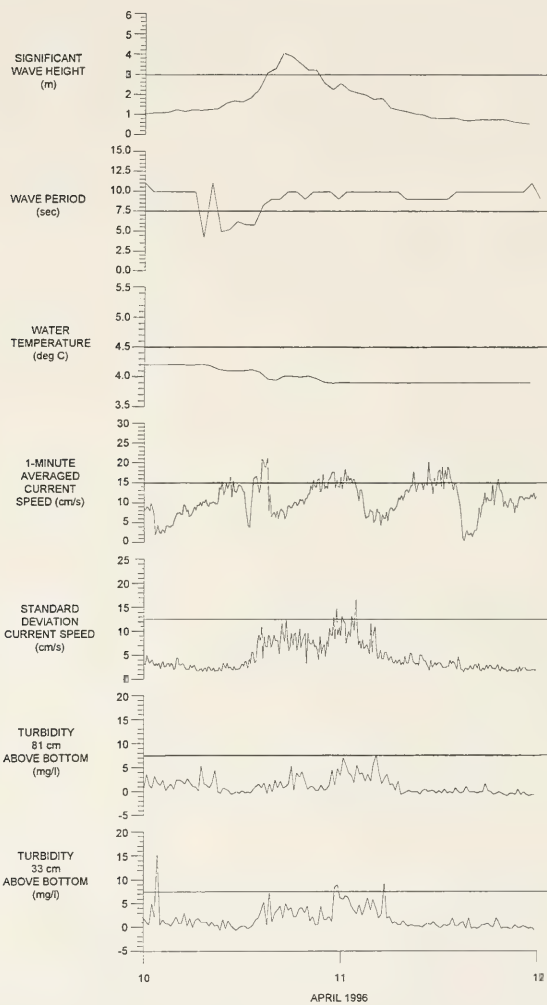


Figure 3-11f. Time series plot of surface wave and near-bottom current and turbidity data during storm 6. The following data are presented on individual tiers starting from the top: significant wave height and peak wave period, near-bottom water temperature, 1-min averaged current speed, the standard deviation in current speed over 1-min periods at 10-min intervals, and turbidity at 81 cm (upper) and 33 cm (lower) above the seafloor.

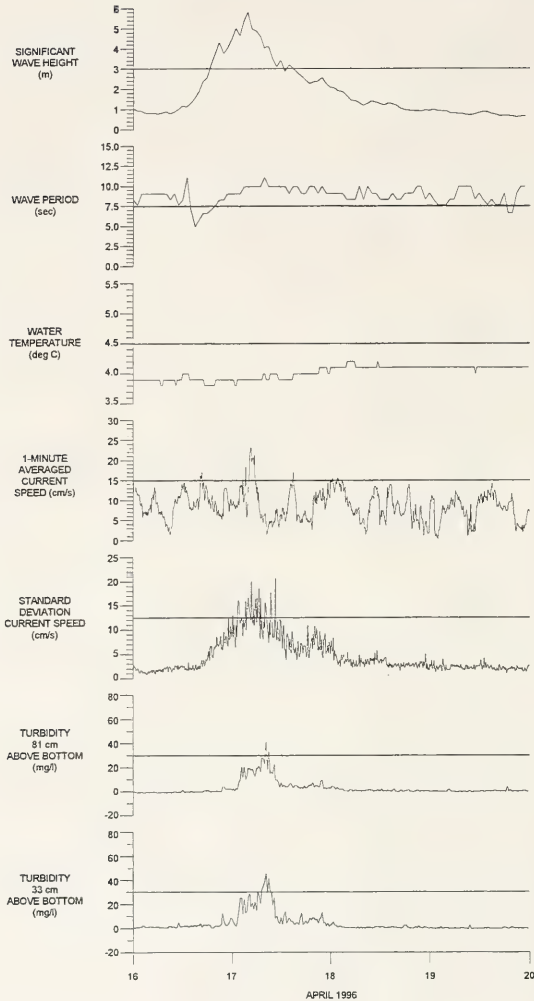


Figure 3-11g. Time series plot of surface wave and near-bottom current and turbidity data during storm 7. The following data are presented on individual tiers starting from the top: significant wave height and peak wave period, near-bottom water temperature, 1-min averaged current speed, the standard deviation in current speed over 1-min periods at 10-min intervals, and turbidity at 81 cm (upper) and 33 cm (lower) above the seafloor.

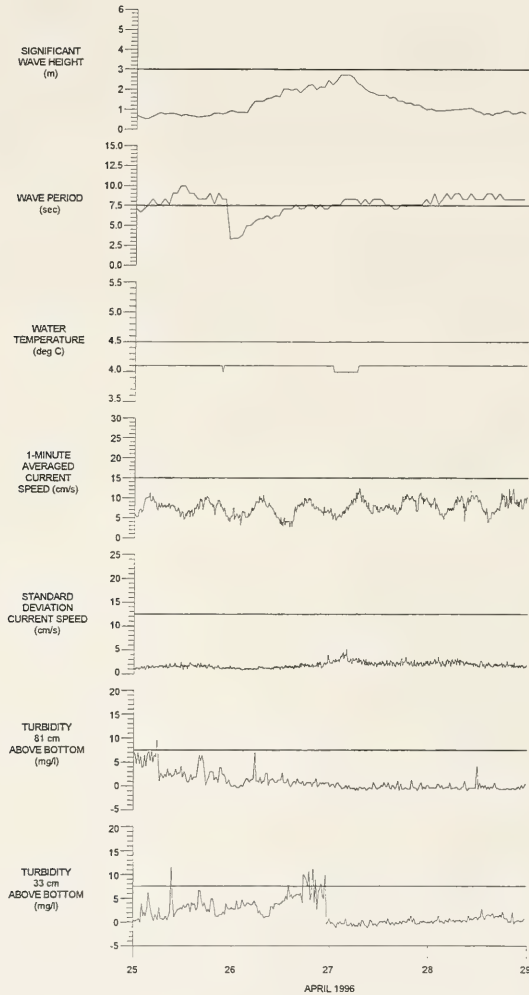


Figure 3-11h. Time series plot of surface wave and near-bottom current and turbidity data during storm 8. The following data are presented on individual tiers starting from the top: significant wave height and peak wave period, near-bottom water temperature, 1-min averaged current speed, the standard deviation in current speed over 1-min periods at 10-min intervals, and turbidity at 81 cm (upper) and 33 cm (lower) above the seafloor.

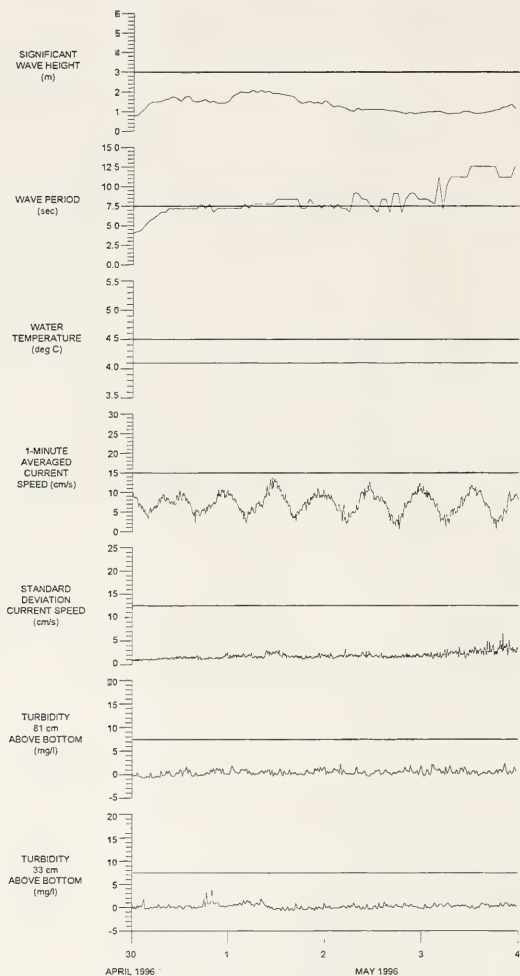


Figure 3-11i. Time series plot of surface wave and near-bottom current and turbidity data during storm 9. The following data are presented on individual tiers starting from the top: significant wave height and peak wave period, near-bottom water temperature, 1-min averaged current speed, the standard deviation in current speed over 1-min periods at 10-min intervals, and turbidity at 81 cm (upper) and 33 cm (lower) above the seafloor.

significant wave heights dropped below roughly 2 m, turbidity levels again approached background levels, suggesting that the suspended material had resettled on the seafloor. We suspect that the short-term events of mildly elevated turbidity levels observed during the two days following storm 3 were due to horizontal advection of slightly turbid water past the moored sensor, rather than isolated events of local sediment resuspension.

Next, we shall investigate the mechanism by which the storm 3 and/or its surface waves caused the apparent resuspension of bottom sediments. Earlier in this section, it was shown that the observed storms had no significant effect on the hourly averaged near-bottom currents in PDS. To further illustrate this point, the middle tier in Figure 3-11c presents the observed near-bottom current speed during storm 3, but for this presentation, the average current speed for each 1-min sampling interval (acquired six times per hour) is shown. Although 1-min averaged current speeds varied from roughly 0 to $20 \text{ cm}\cdot\text{s}^{-1}$ during the four-day record, the major fluctuations occurred at periods of the semi-diurnal tide (12.42 hrs). Minor, high-frequency speed fluctuations occurring early on March 20 may have been due to storm effects, but, overall, storm 3 had no significant effect on currents averaged over durations of 1 min or longer.

Assessment of the potential effects of surface waves on near-bottom currents requires analysis of currents on time scales equivalent to the wave periods (e.g., 5 to 10 sec). Consequently, we must assess the variability in currents within each 1-min sampling interval. Although the 30 current measurements acquired during each sampling interval are insufficient to conduct a spectral analysis of the high-frequency current fluctuations to identify the predominant periods of the current variability, a simple computation of the standard deviation of current speed during each 1-min sampling interval does shed light on the temporal variability in near-bottom current fluctuations that may be driven by surface waves. For example, the third tier from the bottom in Figure 3-11c presents the time series of the standard deviation of near-bottom current speed (SDCS) within each 1-min sampling interval during the 4-day period bracketing storm 3. These results illustrate that SDCS values ranged from background levels near $1 \text{ cm}\cdot\text{s}^{-1}$ prior to the arrival of the storm, to maximum values of approximately $10 \text{ cm}\cdot\text{s}^{-1}$ near the time of maximum near-bottom turbidity. SDCS levels after the storm returned to about $3 \text{ cm}\cdot\text{s}^{-1}$ with slightly more high frequency variability than before the storm. It is also worth noting that the SDCS values were comparable to the magnitude of the 1-min averaged current speeds (i.e., $10\text{-}15 \text{ cm}\cdot\text{s}^{-1}$) during the passage of the storm, such that the maximum instantaneous current speed would be roughly $\frac{1}{2}$ knot ($\approx 25 \text{ cm}\cdot\text{s}^{-1}$): the sum of the mean current ($\approx 10\text{-}15 \text{ cm}\cdot\text{s}^{-1}$) and the standard deviation (SDCS $\approx 15 \text{ cm}\cdot\text{s}^{-1}$). This analysis of SDCS illustrates that the wave-generated, oscillatory, near-bottom currents were responsible for the elevated near-bottom

turbidity levels during storm 3. As the oscillatory currents subsided, the majority of the suspended material apparently resettled to the seafloor (Figure 3-11c).

Similar observations of wave-generated sediment resuspension correlated with high SDCS values are presented in Figures 3-11e, f, and g for storms 5, 6, and 7, respectively. Storm 7 had the largest significant wave heights (5.8 m) of all storms monitored during spring of 1996 (Table 3-4). During this storm (Figure 3-11g) the SDCS reached maximum values of roughly $16 \text{ cm}\cdot\text{s}^{-1}$ shortly after the highest waves were encountered, and near-bottom turbidities approached $40 \text{ mg}\cdot\text{l}^{-1}$ at both sensor levels following the time of most intense SDCS. Wave periods rose to a maximum of roughly 10 s during the time of maximum waves and persisted for approximately 12 hours.

The highest (reliable) near-bottom turbidity levels ($\sim 65 \text{ mg}\cdot\text{l}^{-1}$) during the spring measurement program were encountered during storm 5 although maximum significant wave heights only reached 3.5 m (Figure 3-11e). Wave periods during this storm reached 11.1 s (see Table 3-4) and persisted for more than 24 hours. The duration of elevated SDCS values was much longer during storm 5 than during storm 6, and somewhat longer than during storm 7. We suspect this was due to the relatively long duration of 11 s waves associated with storm 7.

As an additional comment on the apparent differences in sediment resuspension among the relatively strong storms, it is noteworthy that sediment resuspension during storm 6 (maximum of $8 \text{ mg}\cdot\text{l}^{-1}$) was much less than during storm 5 ($65 \text{ mg}\cdot\text{l}^{-1}$) which had comparable maximum significant wave heights (Table 3-5). We suspect that the extended duration of long-period waves of storm 5 (Table 3-4) would cause greater sediment resuspension, but the magnitude of the SDCS values were similar for the two storms, suggesting that the short-term energy was similar during the peak of each storm. It is possible that the relatively lower near-bottom turbidity during storm 6 (Table 3-5) was partially due to a lack of fine-grained sediment available on the seafloor prior to storm 6, which occurred only two days after storm 5. We suspect that, as the time period between storms increases, the amount of fine-grained sediment on the seafloor also will increase due to a combination of normal sediment deposition and aperiodic contributions from lateral transport of dredged material from other locations within PDS. The consistently low, near-bottom, background turbidity levels during the spring measurement program do, however, suggest that little if any dredged material was transported laterally from PDS disposal locations to the site of the moored instrument array.

Table 3-5

Summary of Maximum Wave Heights, Maximum of the Burst-Averaged Standard Deviation in Near-Bottom Current Speeds, Background (Pre-Storm) Concentration of Total Suspended Solids (TSS), Maximum TSS during Storms, and Duration of Elevated TSS during Nine Storm Events during the Period from February 27 to May 14, 1996

Storm Event	Date	Significant Wave Height (m)	Max SDCS ($\text{cm}\cdot\text{s}^{-1}$)	Background TSS Conc. ($\text{mg}\cdot\text{l}^{-1}$)	Max TSS Conc. ($\text{mg}\cdot\text{l}^{-1}$)	Duration Elevated TSS (hrs.)
1	March 8	3.0	10	<1	8	21
2	March 14	3.2	6	<3	3	-
3	March 20	3.6	10	<1	10	12
4	March 26	2.2	2	<3	7	20
5	April 8	3.5	15	<1	65	32
6	April 10	4.0	12	<2	8	33
7	April 16	5.8	16	<3	40	22
8	April 26	2.7	4	<4	9	10
9	May 1	2.0	2	<2	1	-

Summary of Storm Results

The time series data from each of the nine storms (Figures 3-11a through 3-11i) suggest that sediment resuspension is initiated during storms attaining maximum significant wave heights in excess of about 3 m (e.g., storms 1, 3, 5, 6, and 7), whereas significantly elevated turbidity levels were not evident during storms 2, 4, 8, and 9 which had smaller waves. To further assess the potential relationship between wave characteristics and sediment resuspension, the maximum SDCS for each of the nine storms (Table 3-4) has been plotted versus the maximum significant wave height for each storm (Figure 3-12). This presentation illustrates that high-frequency, near-bottom currents (as represented by the SDCS) are correlated with significant wave height at the PDS: for wave heights less than approximately 3 m, maximum SDCS values were less than $8 \text{ cm}\cdot\text{s}^{-1}$ whereas for greater wave heights, SDCS values ranged from roughly 10 to $16 \text{ cm}\cdot\text{s}^{-1}$.

Maximum suspended particulate concentrations during each storm event (Table 3-5) are also shown in Figure 3-12. Although it appears that substantial sediment resuspension occurred during storms 5 and 7 (having suspended particulate concentrations of 65 and $40 \text{ mg}\cdot\text{l}^{-1}$, respectively) when maximum SDCS values exceeded $14 \text{ cm}\cdot\text{s}^{-1}$, one should not assume that SDCS and significant wave height are the only key physical parameters governing sediment resuspension at the PDS. For example, when SDCS values were less

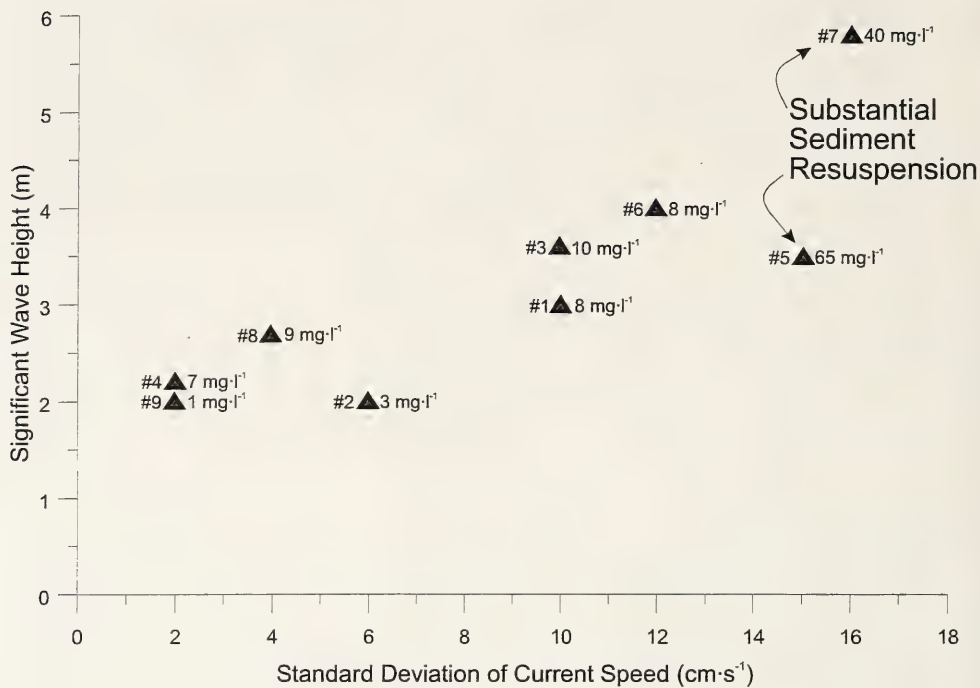


Figure 3-12. Plot illustrating the relationship between maximum significant wave height and the maximum standard deviation in near-bottom current speed for the nine storm events presented in Table 3-4. The maximum suspended particulate concentration also is indicated for each storm.

than $14 \text{ cm}\cdot\text{s}^{-1}$, maximum suspended particulate concentrations varied between 1 and $10 \text{ mg}\cdot\text{l}^{-1}$ with no apparent correlation with significant wave height (Figure 3-12); it is likely that wave period, duration of maximum wave height, and other factors play a major role in the near-bottom energy affecting sediment resuspension. Furthermore, as shown for storms 5 and 6, the availability of fine-grained sediment deposits also plays a role in suspended particulate concentrations in the near-bottom water column.

Also shown in Table 3-5 are the duration of elevated suspended particulate concentrations, the maximum SDCS value, and a comparison of (pre-storm) background and (mid-storm) maximum particulate concentrations for each of the nine storms at PDS. Although these results do not represent a robust dataset for conducting statistical analyses or additional analyses of near-bottom physics, they do reveal the complexity of this multi-parameter problem and contribute valuable information for the design of future measurement programs and/or numerical modeling focused on sediment resuspension at PDS (e.g., Gailani 1997).

4.0 SUMMARY OF MONITORING RESULTS

The Oceanographic Measurement Program conducted in the southwest corner of the Portland Disposal Site (PDS) provided accurate, site-specific data on tides and near-bottom currents, water temperature, and turbidity during the period from late February to mid-May 1996. Measurements were acquired using a bottom-mounted instrument array deployed in a region of relatively rough topography having a water depth of approximately 60 m. Overall, the 78-day measurement program provided excellent data from which to characterize near-bottom currents and turbidity, and evaluate the physical processes governing bottom sediment resuspension within PDS. The wind, wave, and water temperature data obtained from NOAA buoy 44007 located 6 km southwest of PDS were adequate for assessment of the local climatology, as well as meteorological conditions during the current measurement program. The most significant results of the monitoring program are summarized below.

Water Column Characteristics

Vertical profiles of temperature, salinity, and density were acquired at a single location in PDS during three events associated with deployment, servicing, and recovery of the moored instrumentation in February, April, and May 1996, respectively. The February profile revealed a water column that was very weakly stratified, as is typical for the coastal Gulf of Maine in winter. Water property characteristics during late April and mid-May illustrated that relatively fresh and warm water had been introduced to the surface layer, presumably as a result of river discharge. Beneath a moderate thermocline and pycnocline, water properties were nearly constant throughout the lower half of the water column.

With regard to the vertical density stratification, it is apparent that the entire water column to a depth of 60 m is very weakly stratified throughout winter and early spring, whereas the introduction of relatively fresh/warm waters at the surface during mid-spring causes considerable stratification that may tend to decouple horizontal currents and other transport processes within a two-layer water column. Consequently, downward propagation of storm-generated energy would be most effective during winter and late spring when the water column is nearly void of density stratification. With the onset of spring and summer, the bottom waters will be less free to mix vertically with the upper layers, and the resulting stratification may act as a partial barrier to the energy imparted by storms.

Surface Wave Climatology

Time-series observations of winds, atmospheric pressure, surface water temperature, and waves from NOAA buoy 44007 were analyzed to assess seasonal and inter-annual variability in meteorological conditions at PDS from January 1993 through May 1996.

Analysis of the annual wave statistics revealed that wave characteristics were very similar for the 3.4 years of wave records, and significant wave heights less than 2 m occurred from 90 to 95% of the time during each year. The maximum significant wave height observed in each of the four measurement years ranged from 5.6 to 7.3 m. Overall, wave characteristics during the first half of 1996 were typical of other recent years at this location.

Analysis of the seasonal variability in wave conditions at PDS revealed that mean significant wave heights were 1.2 m in winter (December through February), approximately 1 m in spring and fall, and 0.7 m in summer (June through August). Mean wave periods were approximately 8 sec during all seasons, with a standard deviation of approximately 3 sec. Maximum significant wave heights were roughly 3 m in summer, compared to 6 m in winter, and 7 m in spring and fall. Significant wave heights greater than 3 m were observed over 4% of the time in winter, compared to 2% in spring and fall, and 0% in summer.

The duration of large waves during the passage of major storms is relatively brief, often persisting for only a fraction of a day. Quantitative analysis of storm waves revealed 72 events during the 3.4-year analysis period that had significant wave heights between 3 and 4 m; average durations for these events were only 6 to 8 hrs. Wave heights in the range of 5 to 6 m were observed only 22 times; average durations were only 1 to 3 hrs, for a total of 59 cumulative hours over the 3.4 years.

The wave records from March through May 1996 exhibited nine storm events attaining significant wave heights greater than 2 m, with one reaching 5.8 m. This storm activity was similar to that during other recent years, and sufficient for analysis of storm-generated currents as they affect bottom sediment resuspension.

Near-Bottom Currents

The three consecutive deployments of moored instrumentation at PDS yielded nearly complete records of near-bottom currents, water temperature, pressure, and relative turbidity over the period from late February to mid-May 1996. Hourly averaged near-bottom current speeds during the measurement period ranged from approximately 0 to 20 $\text{cm}\cdot\text{s}^{-1}$, with the majority of the variability occurring at periods of approximately 12 hr in association with the semi-diurnal tide.

The mean current speed for each of the three deployments was very consistent ($7.0 \pm 0.4 \text{ cm}\cdot\text{s}^{-1}$), but the mean direction varied greatly among the deployments, presumably due to rough topography (e.g., boulders and rock ledges) in close proximity to the moored instrumentation.

Tidal harmonic analysis of the current velocity data revealed that near-bottom tidal currents at this location are very weak and predominantly driven by the M_2 semi-diurnal constituent having a period of 12.42 hrs. The amplitude of the M_2 current was approximately $3 \text{ cm}\cdot\text{s}^{-1}$, compared to less than $0.5 \text{ cm}\cdot\text{s}^{-1}$ for all other constituents. At this location, the M_2 tidal current rotates in a counter-clockwise direction around an ellipse having a major axis oriented roughly east-west.

Analysis of residual currents (after the mean current and the tidal currents had been removed from the observed records) revealed that storms had almost no effect on the hourly averaged near-bottom currents at PDS. This result is consistent with prior studies in the Gulf of Maine which showed that currents are not coherent with local winds or coastal pressure fluctuations during the passage of storms.

Near-Bottom Turbidity

Time-series measurements of turbidity during the 78-day measurement period were acquired using optical sensors at levels of 33 and 81 cm above the seafloor. Both sensors provided excellent quality data with no appreciable biofouling such that turbidity fluctuations above a consistently low (less than $2 \text{ mg}\cdot\text{l}^{-1}$) background level could be distinguished.

Storm Effects on Near-Bottom Currents and Turbidity

The near-bottom turbidity data acquired during the nine storm events having significant wave heights greater than 2 m (from late February through mid-May 1996) revealed that sediment resuspension was substantial during two storms, both of which had significant wave heights in excess of 3 m. Analysis of the near-bottom current data during these storms revealed that high-frequency oscillatory currents were induced by the storm waves such that instantaneous (1-sec) current speeds reached approximately $\frac{1}{2}$ knot ($25 \text{ cm}\cdot\text{s}^{-1}$) as the large waves passed over the measurement site. The burst sampling scheme of the internally recording current meter was insufficient to allow spectral analysis of wave-induced current fluctuations, but the standard deviation of current speed (SDCS) within 1-min sampling periods (during which 30 samples were acquired at 0.5 Hz intervals) revealed that intensified currents occurred simultaneously with observations of high near-bottom turbidity during the most intense storms.

Although the available data acquired during the moored instrument program and from NOAA buoy 44007 are insufficient to derive a quantitative relationship between wave characteristics (height, period, duration, and incident direction), near-bottom currents and bottom stress, and sediment resuspension at PDS, the results presented herein are very useful for 1) validation of hindcast models of storm-induced sediment resuspension (Gailani 1997), and 2) design of more ambitious measurement and analysis programs to evaluate wave-induced bottom stress and sediment resuspension under a variety of wave conditions.

5.0 REFERENCES

- Brown, W. S.; Beardsley, R. C. 1978. Winter circulation in the western Gulf of Maine: Part 1. Cooling and water mass formation. *Journal of Physical Oceanography*. Vol 8. pp 265-277.
- Colton, J. B.; Marak, R. R.; Nickerson, S.; Stoddard, R. 1968. Physical, chemical, and biological observations on the continental shelf, Nova Scotia to Long Island, 1964-66. U.S. Fish Wildlife Serv. Data Rep. No. 23, 190 pp.
- EPA. 1987. Final rulemaking designation of Portland, Maine, dredged material disposal site, Region I. US Environmental Protection Agency, Region I, JFK Federal Building, Boston, MA, September 16, 1987.
- Gailani, J. Z. 1997. Sediment erosion modeling at the Portland Disposal Site. Report submitted to US Army Corps of Engineers, New England Division, Waltham, MA.
- Hopkins, T.; Garfield, N. 1977. The existence of Maine intermediate water. A summary of an informal workshop of the Gulf of Maine and adjacent seas. WHOI Spec. Rep., 52 pp.
- Morris, J. 1996. DAMOS site management plans. SAIC Report No. 365. Final report submitted to US Army Corps of Engineers, New England Division, Waltham, MA.
- Naval Underwater Systems Center. 1979. DAMOS Disposal Area Monitoring System annual data report - 1978. Supplement B, Portland Disposal Site. Submitted to US Army Corps of Engineers, New England Division, Waltham, MA.
- SAIC. 1995a. Sediment capping of subaqueous dredged material disposal mounds: An overview of the New England experience, 1979-1993. DAMOS Contribution No. 95 (SAIC Report No. SAIC-90/7573&C84). US Army Corps of Engineers, New England Division, Waltham, MA.
- SAIC. 1995b. Portland Disposal Site capping demonstration study: Baseline survey results. SAIC Report No. 355. Draft report submitted to US Army Corps of Engineers, New England Division, Waltham, MA.
- Vermersch, J. A.; Beardsley, R. C.; Brown, W. S. 1979. Winter circulation in the western Gulf of Maine: Part 2. Current and pressure observations. *Journal of Physical Oceanography*. Vol 9. pp 768-784.

Wiley, M. B. 1996. Monitoring cruise at the Portland Disposal Site, July 1992. DAMOS Contribution No. 108 (SAIC Report No. C110). US Army Corps of Engineers, New England Division, Waltham, MA.

INDEX

buoy, ii, iv, v, vi, viii, 3, 8, 13, 20, 24, 26, 27, 28, 30, 39, 58, 60

capping, 1, 3, 61

circulation, 61

conductivity, 8, 13

CTD meter, 13, 31, 33

currents, ii, v, vi, viii, ix, x, 1, 3, 5, 8, 11, 17, 20, 24,

30, 33, 35, 36, 39, 41, 53, 55, 58, 59, 60

direction, 31, 35

meter, 9, 31, 35, 39, 60

speed, vii, ix, 11, 31, 39, 41, 53, 59, 60

decomposition, 33

density, v, viii, 13, 14, 17, 58

sigma-t, v, 14

deposition, 54

disposal site

Portland (PDS), v, viii, ix, x, 1, 3, 5, 6, 8, 9, 13, 14,

17, 20, 24, 27, 28, 30, 36, 39, 41, 53, 54, 55, 57,

58, 59, 60, 61, 62

erosion, x, 5, 61

fish, 61

National Oceanic and Atmospheric Administration

(NOAA), ii, iv, v, vi, viii, 3, 13, 20, 24, 26, 28, 30,

39, 58, 60

resuspension, viii, ix, x, 1, 3, 5, 20, 24, 43, 53, 54, 55,

57, 58, 59, 60

salinity, v, viii, 14, 17, 58

sediment

clay, 3, 9

gravel, 3, 9, 11

resuspension, viii, ix, x, 1, 3, 5, 20, 24, 43, 53, 54, 55, 57, 58, 59, 60

sand, 3, 8, 9, 11

silt, 3, 8, 9, 11

sediment sampling

grabs, ii, 9

species

dominance, 20, 24, 31

statistical testing, ii, iv, viii, 13, 24, 26, 27, 28, 36, 57, 59

survey

baseline, 61

bathymetry, v, 3, 6, 8, 31

suspended sediment, 43

temperature, v, vi, viii, ix, 5, 8, 9, 11, 13, 14, 17, 20,

24, 30, 31, 33, 35, 41, 58, 59

thermocline, viii, 17, 31, 58

tide, vi, viii, ix, 3, 5, 11, 31, 33, 35, 36, 39, 53, 58,

59, 60

topography, viii, ix, 3, 6, 8, 35, 39, 58, 59

trace metals

arsenic (As), 1, 8, 9, 11, 14, 27, 28, 35, 36, 39, 41, 43, 54

vanadium (V), 33, 36

zinc (Zn), 9, 61

turbidity, ii, v, vi, vii, viii, ix, x, 3, 5, 9, 11, 13, 30,

39, 41, 43, 53, 54, 55, 58, 59, 60

turbulence, 9

waves, ii, iv, v, vi, vii, viii, ix, x, 3, 5, 13, 20, 24, 26,

27, 28, 30, 39, 41, 43, 53, 54, 55, 57, 58, 59, 60

APPENDIX A

ANNUAL WAVE STATISTICS

A-2 Annual Statistics - 1994

FREQUENCY DISTRIBUTION
1.00 HOURLY DATA

SPANNING 1/1/94 TO 12/31/94

STATION: 44007A

8094 DATA POINTS - 92.4 PERCENT OF TOTAL

PEAK WAVE PERIOD SEC	PERCENT	MEAN HEIGHT	MIN HEIGHT	MAX HEIGHT	STD. DEV.	
1- 2	0.1	0.20	0.10	0.40	0.51	
2- 3	2.5	0.40	0.10	0.80	0.30	
3- 4	7.0	0.61	0.20	1.97	0.00	
4- 5	9.2	0.76	0.20	1.90	0.32	
5- 6	15.8	0.82	0.20	2.30	0.51	
6- 7	9.9	0.95	0.20	2.74	0.60	
7- 8	12.5	0.90	0.20	3.30	0.58	
8- 9	8.6	0.80	0.20	3.60	0.52	
9- 10	9.2	0.82	0.20	4.50	0.61	
10- 11	9.8	1.00	0.14	4.70	0.82	
11- 12	8.5	1.19	0.12	5.60	1.06	
12- 13	4.4	1.03	0.20	4.60	0.94	
13- 14	0.1	2.36	1.03	3.14	0.63	
14- 15	1.9	0.94	0.20	4.60	1.20	
15- 16	0.0	0.00	0.00	0.00	0.00	
16- 17	0.7	0.32	0.20	0.50	0.39	
17- 18	0.0	0.00	0.00	0.00	0.00	
18- 19	0.0	0.00	0.00	0.00	0.00	
19- 20	0.0	0.00	0.00	0.00	0.00	
HEIGHT	0	1	2	3	4	5
M	1	1	1	1	1	1
	1	2	3	4	5	6
PERCENT	68.6	26.2	3.8	0.8	0.4	0.1
MEAN PK HV PER	7	8	10	11	11	11
STD DEV	3	3	3	3	3	3
100.00						

SUMMARY STATISTICS

MEAN HEIGHT= 0.88 M STANDARD DEVIATION = 0.60 M MAXIMUM = 5.60 M MINIMUM = 0.10 M RANGE = 5.50 M
 SKENNESS = 0.88 M SKENNESS = 2.59

IN A COORDINATE SYSTEM WHOSE Y AXIS IS POSITIONED 0.00 DEGREES CLOCKWISE FROM TRUE NORTH
 MEAN X COMPONENT = 0.88 M STANDARD DEVIATION = 0.60 M SKENNESS = 2.59
 MEAN Y COMPONENT = 7.57 SEC STANDARD DEVIATION = 2.83 SEC SKENNESS = 0.42

A-3 Annual Statistics - 1995

FREQUENCY DISTRIBUTION
1.00 HOURLY DATA

STATION: 44007A

SPANNING 1/ 1/95 TO 12/31/95

7858 DATA POINTS - 89.7 PERCENT OF TOTAL

PEAK WAVE PERIOD SEC	PERCENT	MEAN HEIGHT	MIN HEIGHT	MAX HEIGHT	STD. DEV.
2- 3	1.9	0.0	0.0	0.0	0.26
3- 4	5.7	0.3	0.0	0.0	0.00
4- 5	5.8	1.7	0.0	0.0	0.00
5- 6	5.4	4.8	0.1	0.0	0.34
6- 7	4.3	3.1	0.6	0.0	0.56
7- 8	6.0	2.7	1.0	0.2	0.64
8- 9	5.8	2.4	0.5	0.0	0.74
9- 10	6.9	4.3	0.7	0.2	0.70
10- 11	7.3	4.5	0.4	0.1	0.84
11- 12	6.3	3.9	0.6	0.1	0.76
12- 13	4.0	2.7	0.6	0.1	0.93
13- 14	0.0	0.0	0.0	0.0	1.33
14- 15	1.5	1.2	0.1	0.0	0.65
15- 16	0.0	0.0	0.0	0.0	0.00
16- 17	0.1	0.6	0.1	0.0	0.00
17- 18	0.0	0.0	0.0	0.0	0.00
18- 19	0.0	0.0	0.0	0.0	0.00
19- 20	0.0	0.1	0.0	0.0	0.00

HEIGHT 0 1 2 3 4 5 6 7
M 1 1 1 1 1 1 1 1

PERCENT 61.4 32.5 4.7 1.0 0.3 0.2 0.1 0.0
MEAN PK WV PER 8 9 9 10 10 11 11 13
STD DEV 4 3 3 3 3 3 3 0

100.00

SUMMARY STATISTICS

MEAN HEIGHT = 0.96 M STANDARD DEVIATION = 0.63 M MAXIMUM = 7.30 M MINIMUM = 0.20 M RANGE = 7.10 M
SKENNESS = 2.64

IN A COORDINATE SYSTEM WHOSE Y AXIS IS POSITIONED 0.00 DEGREES CLOCKWISE FROM TRUE NORTH
MEAN X COMPONENT = 0.96 M STANDARD DEVIATION = 0.63 M SKENNESS = 2.64
MEAN Y COMPONENT = 6.29 SEC STANDARD DEVIATION = 2.94 SEC SKENNESS = 0.13

A-4 Statistics: January - May 1996

FREQUENCY DISTRIBUTION
1.00 HOURLY DATA

STATION: 44007A

SPANNING 1/ 1/96 TO 5/31/96

3648 DATA POINTS - 100.0 PERCENT OF TOTAL

PEAK WAVE PERIOD
SEC

PERCENT	MEAN HEIGHT	MIN HEIGHT	MAX HEIGHT	STD. DEV.
2- 3	2.4	0.0	0.0	0.0
3- 4	6.6	0.7	0.0	0.0
4- 5	4.4	2.5	0.0	0.0
5- 6	3.2	5.0	0.2	0.0
6- 7	2.7	4.0	0.8	0.0
7- 8	4.0	5.2	1.9	0.2
8- 9	5.2	3.2	0.7	0.3
9- 10	6.4	4.3	1.4	0.4
10- 11	7.6	5.8	1.0	0.3
11- 12	6.4	4.6	0.8	0.4
12- 13	3.2	2.1	0.1	0.0
13- 14	0.0	0.0	0.0	0.0
14- 15	0.5	0.1	0.0	0.0

HEIGHT	0	1	2	3	4	5
M	1	1	1	1	1	1
	1	2	3	4	5	6

MEAN PK WV PER 8 8 8 8 8 8 8
STD DEV 4 3 3 3 3 3 3

SUMMARY STATISTICS

MEAN HEIGHT = 1.09 M STANDARD DEVIATION = 0.73 M MINIMUM = 0.18 M RANGE = 5.62 M
STANDARD DEVIATION = 0.73 M SKEWNESS = 1.94

IN A COORDINATE SYSTEM WHOSE Y AXIS IS POSITIONED 0.00 DEGREES CLOCKWISE FROM TRUE NORTH
MEAN X COMPONENT = 1.09 M STANDARD DEVIATION = 0.73 M SKEWNESS = 1.94
MEAN Y COMPONENT = 8.06 SEC STANDARD DEVIATION = 2.69 SEC SKEWNESS = -0.26

100.00

A-5 Multi-year Statistics: January 1993 - May 1996

FREQUENCY DISTRIBUTION
1.00 HOURLY DATA

STATION: 44007A

SPANNING 1/ 1 TO 12/31 YEARS: 1993 - 1996

27743 DATA POINTS - 94.7 PERCENT OF TOTAL

PEAK WAVE PERIOD SEC	PERCENT	MEAN HEIGHT	MIN HEIGHT	MAX HEIGHT	STD. DEV.
0- 1	0.0	0.00	0.00	0.00	0.00
1- 2	0.0	0.00	0.10	0.40	0.51
2- 3	1.6	0.42	0.10	0.90	0.27
3- 4	5.3	0.62	0.20	2.27	0.00
4- 5	5.8	0.77	0.20	1.90	0.35
5- 6	5.9	0.99	0.20	2.40	0.53
6- 7	4.3	1.06	0.20	2.90	0.65
7- 8	7.2	1.02	0.18	3.90	0.71
8- 9	6.2	0.92	0.20	4.60	0.68
9- 10	7.6	0.97	0.19	6.00	0.83
10- 11	7.4	1.04	0.14	6.30	0.90
11- 12	5.8	1.15	0.12	7.00	0.95
12- 13	3.1	1.19	0.20	7.30	1.04
13- 14	2.1	1.09	0.20	5.90	1.12
14- 15	1.3	2.72	1.35	4.10	2.77
15- 16	0.0	0.94	0.20	4.60	0.91
16- 17	0.3	0.00	0.00	0.00	0.00
17- 18	0.0	0.00	0.00	0.00	0.00
18- 19	0.0	0.00	0.00	0.00	0.00
19- 20	0.0	0.00	0.00	0.00	0.00

HEIGHT M	0	1	2	3	4	5	6
PERCENT	61.8	30.7	5.3	1.3	0.6	0.2	0.0
MEAN PK WV PER	8	9	10	11	11	11	
STD DEV	3	3	3	3	3	3	3

SUMMARY STATISTICS

MEAN HEIGHT = 0.98 M STANDARD DEVIATION = 0.69 M RANGE = 7.20 M
 MAXIMUM = 7.30 M MINIMUM = 0.10 M

IN A COORDINATE SYSTEM WHOSE Y AXIS IS POSITIONED 0.00 DEGREES CLOCKWISE FROM TRUE NORTH
 MEAN X COMPONENT = 0.98 M STANDARD DEVIATION = 0.69 M
 MEAN Y COMPONENT = 8.10 SEC STANDARD DEVIATION = 2.78 SEC

100.00

APPENDIX B

SEASONAL WAVE STATISTICS

B-1 Winter Statistics for 1994, 1995, 1996 (December - February)

FREQUENCY DISTRIBUTION
1.00 HOURLY DATA

STATION: 44007A

SPANNING 12/ 1 TO 2/28 YEARS: 1992 - 1996

6036 DATA POINTS - 82.9 PERCENT OF TOTAL

PEAK WAVE PERIOD SEC	0- 1	1- 2	2- 3	3- 4	4- 5	5- 6	6- 7	7- 8	8- 9	9- 10	10- 11	11- 12	12- 13	13- 14	14- 15	15- 16	16- 17	17- 18	18- 19	19- 20	PERCENT	MEAN HEIGHT	MIN HEIGHT	MAX HEIGHT	STD. DEV.
	0.0	0.0	0.0	0.0	0.0	0.0	0.0	0.0	0.0	0.0	0.0	0.0	0.0	0.0	0.0	0.0	0.0	0.0	0.0	0.0	0.0	0.00	0.10	0.40	0.00
	0.1	0.0	0.0	0.0	0.0	0.0	0.0	0.0	0.0	0.0	0.0	0.0	0.0	0.0	0.0	0.0	0.0	0.0	0.0	0.0	0.1	0.20	0.10	0.40	0.51
	2.4	0.0	0.0	0.0	0.0	0.0	0.0	0.0	0.0	0.0	0.0	0.0	0.0	0.0	0.0	0.0	0.0	0.0	0.0	0.0	2.4	0.43	0.20	0.90	0.25
	8.6	0.6	0.0	0.0	0.0	0.0	0.0	0.0	0.0	0.0	0.0	0.0	0.0	0.0	0.0	0.0	0.0	0.0	0.0	0.0	9.2	0.65	0.20	1.97	0.06
	5.4	3.1	0.0	0.0	0.0	0.0	0.0	0.0	0.0	0.0	0.0	0.0	0.0	0.0	0.0	0.0	0.0	0.0	0.0	0.0	8.5	0.88	0.30	1.90	0.46
	3.9	6.0	0.3	0.0	0.0	0.0	0.0	0.0	0.0	0.0	0.0	0.0	0.0	0.0	0.0	0.0	0.0	0.0	0.0	0.0	10.2	1.14	0.20	2.30	0.56
	1.6	3.6	1.3	0.0	0.0	0.0	0.0	0.0	0.0	0.0	0.0	0.0	0.0	0.0	0.0	0.0	0.0	0.0	0.0	0.0	6.5	1.41	0.20	2.90	0.72
	1.5	3.2	2.2	0.2	0.0	0.0	0.0	0.0	0.0	0.0	0.0	0.0	0.0	0.0	0.0	0.0	0.0	0.0	0.0	0.0	7.0	1.58	0.20	3.70	0.89
	1.9	1.9	1.0	0.2	0.0	0.0	0.0	0.0	0.0	0.0	0.0	0.0	0.0	0.0	0.0	0.0	0.0	0.0	0.0	0.0	5.1	1.37	0.20	4.60	0.96
	4.3	3.3	1.8	0.3	0.2	0.0	0.0	0.0	0.0	0.0	0.0	0.0	0.0	0.0	0.0	0.0	0.0	0.0	0.0	0.0	10.0	1.36	0.20	6.00	1.05
	7.1	5.1	1.4	0.7	0.4	0.1	0.0	0.0	0.0	0.0	0.0	0.0	0.0	0.0	0.0	0.0	0.0	0.0	0.0	0.0	14.7	1.28	0.20	5.60	1.09
	6.3	3.3	1.2	0.5	0.0	0.0	0.0	0.0	0.0	0.0	0.0	0.0	0.0	0.0	0.0	0.0	0.0	0.0	0.0	0.0	16.4	1.34	0.20	5.60	1.07
	0.0	0.0	0.0	0.0	0.0	0.0	0.0	0.0	0.0	0.0	0.0	0.0	0.0	0.0	0.0	0.0	0.0	0.0	0.0	0.0	8.4	1.32	0.20	4.40	1.00
	0.5	0.2	0.3	0.2	0.1	0.0	0.0	0.0	0.0	0.0	0.0	0.0	0.0	0.0	0.0	0.0	0.0	0.0	0.0	0.0	0.1	2.36	1.03	3.14	0.63
	0.0	0.0	0.0	0.0	0.0	0.0	0.0	0.0	0.0	0.0	0.0	0.0	0.0	0.0	0.0	0.0	0.0	0.0	0.0	0.0	1.3	1.91	0.30	4.60	1.30
	0.1	0.0	0.0	0.0	0.0	0.0	0.0	0.0	0.0	0.0	0.0	0.0	0.0	0.0	0.0	0.0	0.0	0.0	0.0	0.0	0.1	0.00	0.00	0.00	0.00
	0.0	0.0	0.0	0.0	0.0	0.0	0.0	0.0	0.0	0.0	0.0	0.0	0.0	0.0	0.0	0.0	0.0	0.0	0.0	0.0	0.0	0.28	0.20	0.30	0.44
	0.0	0.0	0.0	0.0	0.0	0.0	0.0	0.0	0.0	0.0	0.0	0.0	0.0	0.0	0.0	0.0	0.0	0.0	0.0	0.0	0.0	0.00	0.00	0.00	0.00
	0.0	0.0	0.0	0.0	0.0	0.0	0.0	0.0	0.0	0.0	0.0	0.0	0.0	0.0	0.0	0.0	0.0	0.0	0.0	0.0	0.0	0.00	0.00	0.00	0.00
	0.0	0.0	0.0	0.0	0.0	0.0	0.0	0.0	0.0	0.0	0.0	0.0	0.0	0.0	0.0	0.0	0.0	0.0	0.0	0.0	0.0	0.00	0.00	0.00	0.00

100.00

SUMMARY STATISTICS

MEAN HEIGHT = 1.22 STANDARD DEVIATION = 0.83 RANGE = 5.90
 MAXIMUM = 6.00 MINIMUM = 0.10

IN A COORDINATE SYSTEM WHOSE Y AXIS IS POSITIONED 0.00 DEGREES CLOCKWISE FROM TRUE NORTH
 MEAN X COMPONENT = 1.22 STANDARD DEVIATION = 0.83
 MEAN Y COMPONENT = 8.16 STANDARD DEVIATION = 3.03

B-2 Spring Statistics for 1993, 1994, 1995, 1996 (March - May)

FREQUENCY DISTRIBUTION

1.00 HOURLY DATA

STATION: 44007A

SPANNING 3/ 1 TO 5/31 YEARS: 1993 - 1996

8507 DATA POINTS - 96.3 PERCENT OF TOTAL

PEAK WAVE PERIOD
SEC

PERCENT	MEAN HEIGHT	MIN HEIGHT	MAX HEIGHT	STD. DEV.
0- 1	0.0	0.0	0.0	0.0
1- 2	0.0	0.0	0.0	0.0
2- 3	1.1	0.0	0.0	0.0
3- 4	3.7	0.3	0.0	0.0
4- 5	3.8	1.7	0.0	0.0
5- 6	4.4	5.8	0.1	0.0
6- 7	3.6	4.2	0.5	0.0
7- 8	5.9	5.7	1.0	0.0
8- 9	7.0	3.8	0.4	0.2
9- 10	9.0	4.5	0.6	0.2
10- 11	7.8	5.4	0.8	0.4
11- 12	5.3	3.6	0.5	0.1
12- 13	2.5	2.1	0.6	0.1
13- 14	0.0	0.1	0.0	0.0
14- 15	0.7	0.4	0.2	0.1
15- 16	0.0	0.0	0.0	0.0
16- 17	0.1	0.0	0.0	0.0
17- 18	0.0	0.0	0.0	0.0
18- 19	0.0	0.0	0.0	0.0
19- 20	0.0	0.0	0.0	0.0

HEIGHT	0	1	2	3	4	5	6
M	!	!	!	!	!	!	!
PERCENT	55.0	37.7	4.8	1.3	0.9	0.3	0.0
MEAN PK WV PER	8	10	10	11	12	12	
STD DEV	3	3	3	3	3	3	

100.00

SUMMARY STATISTICS

MEAN HEIGHT = 1.06 M STANDARD DEVIATION = 0.70 M MAXIMUM = 7.00 M MINIMUM = 0.18 M RANGE = 6.82 M

IN A COORDINATE SYSTEM WHOSE Y AXIS IS POSITIONED 0.00 DEGREES CLOCKWISE FROM TRUE NORTH
 MEAN X COMPONENT = 1.06 M STANDARD DEVIATION = 0.70 M
 MEAN Y COMPONENT = 8.27 SEC STANDARD DEVIATION = 2.52 SEC
 STANDARD DEVIATION = 2.78 SEC

B-3 Summer Statistics for 1993, 1994, 1995 (June - August)

FREQUENCY DISTRIBUTION

1.00 HOURLY DATA

STATION: 44007A

SPANNING 6/ 1 TO 8/31 YEARS: 1993 - 1996

6624 DATA POINTS - 100.0 PERCENT OF TOTAL

PEAK HAVE PERIOD
SEC

PERCENT	MEAN HEIGHT	MIN HEIGHT	MAX HEIGHT	STD. DEV.
0- 1	0.0	0.0	0.0	0.0
1- 2	0.0	0.0	0.0	0.0
2- 3	0.6	0.0	0.0	0.0
3- 4	3.6	0.0	0.0	0.0
4- 5	8.3	1.0	0.0	0.0
5- 6	10.3	3.5	0.0	0.0
6- 7	9.3	2.1	0.1	0.0
7- 8	16.8	2.1	0.1	0.0
8- 9	10.3	1.5	0.0	0.0
9-10	8.5	1.6	0.0	0.0
10-11	7.2	1.3	0.0	0.0
11-12	4.0	1.1	0.0	0.0
12-13	2.7	1.1	0.1	0.0
13-14	0.0	0.0	0.0	0.0
14-15	1.9	0.5	0.1	0.0
15-16	0.0	0.0	0.0	0.0
16-17	0.1	0.2	0.1	0.0
17-18	0.0	0.0	0.0	0.0
18-19	0.0	0.0	0.0	0.0
19-20	0.0	0.0	0.0	0.0

HEIGHT 0 1 2 3 4 5 6 7

M 1 2 3 4 5 6 7 3

PERCENT 81.4 16.0 0.5 0.0 0.0 0.0 0.0

MEAN PK WV PER 8 11 0 0 0 0 0

STD DEV 3 3 4 0 0 0 0

100.00

SUMMARY STATISTICS

MEAN HEIGHT = 0.68

STANDARD DEVIATION = 0.32

MINIMUM = 0.20

RANGE = 2.50

IN A COORDINATE SYSTEM WHOSE Y AXIS IS POSITIONED 0.00 DEGREES CLOCKWISE FROM TRUE NORTH

MEAN X COMPONENT = 0.68

STD DEV COMPONENT = 7.69

STANDARD DEVIATION = 0.32

STANDARD DEVIATION = 2.50

